Luise Theil Kuhn
Head of Section “Imaging and Structural Analysis”, DTU Energy

Neutron Imaging

Motivation

This module's important concepts

- Instrumentation
- Radiography (2D)
- Tomography (3D)
- In situ/In operando
- Virtual Imaging experiment

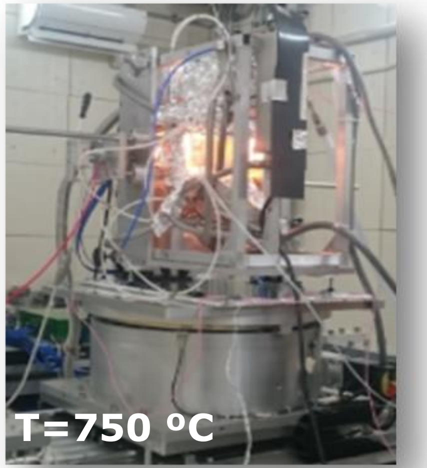

Image and contrast formation

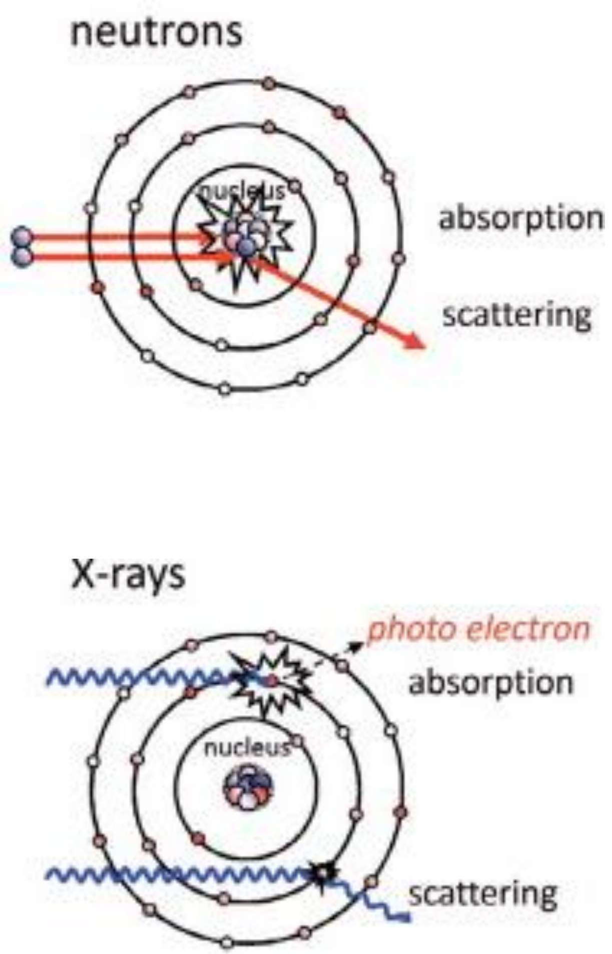

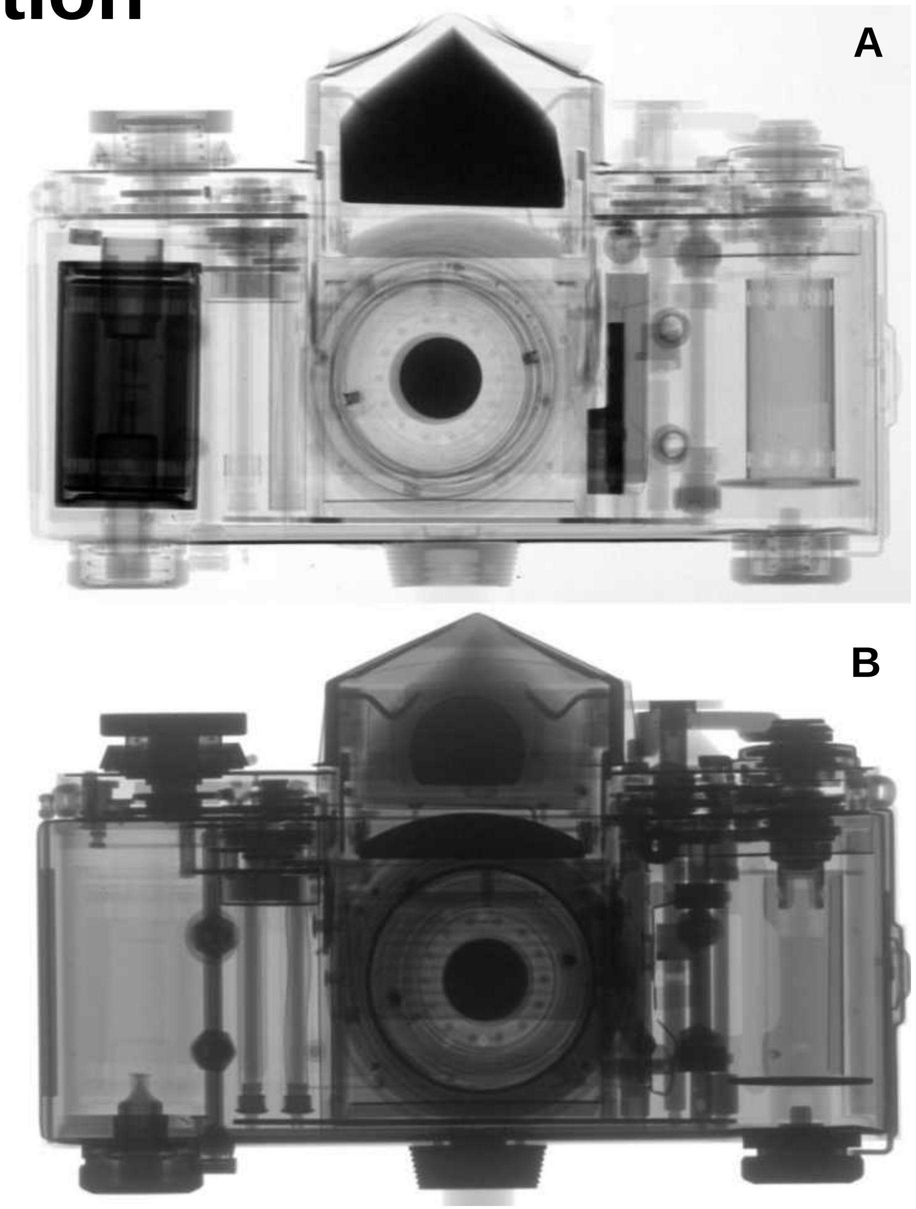

Image and contrast formation

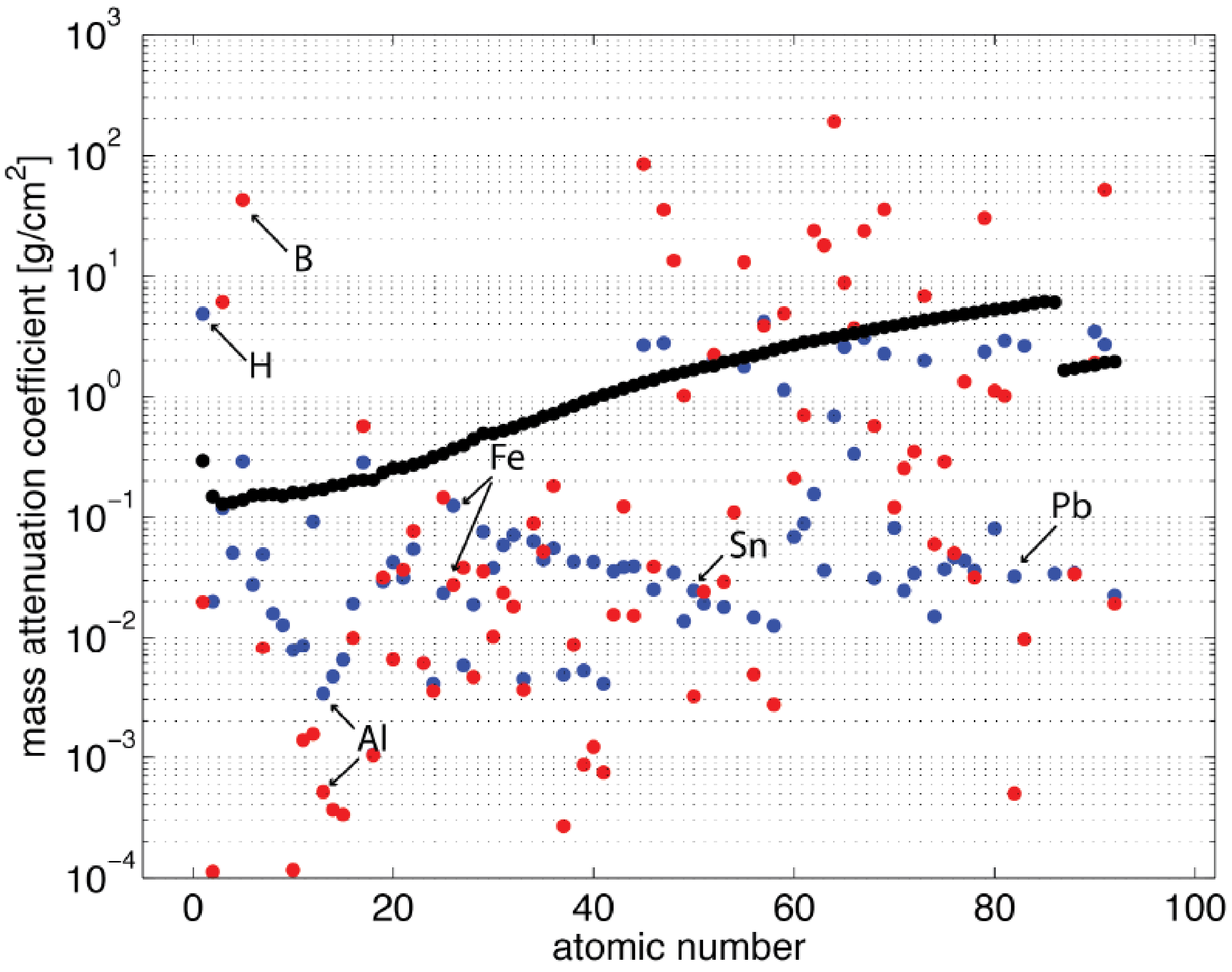

$$\frac{\mu}{\rho} = \frac{N_a}{M}\sigma$$

Summary

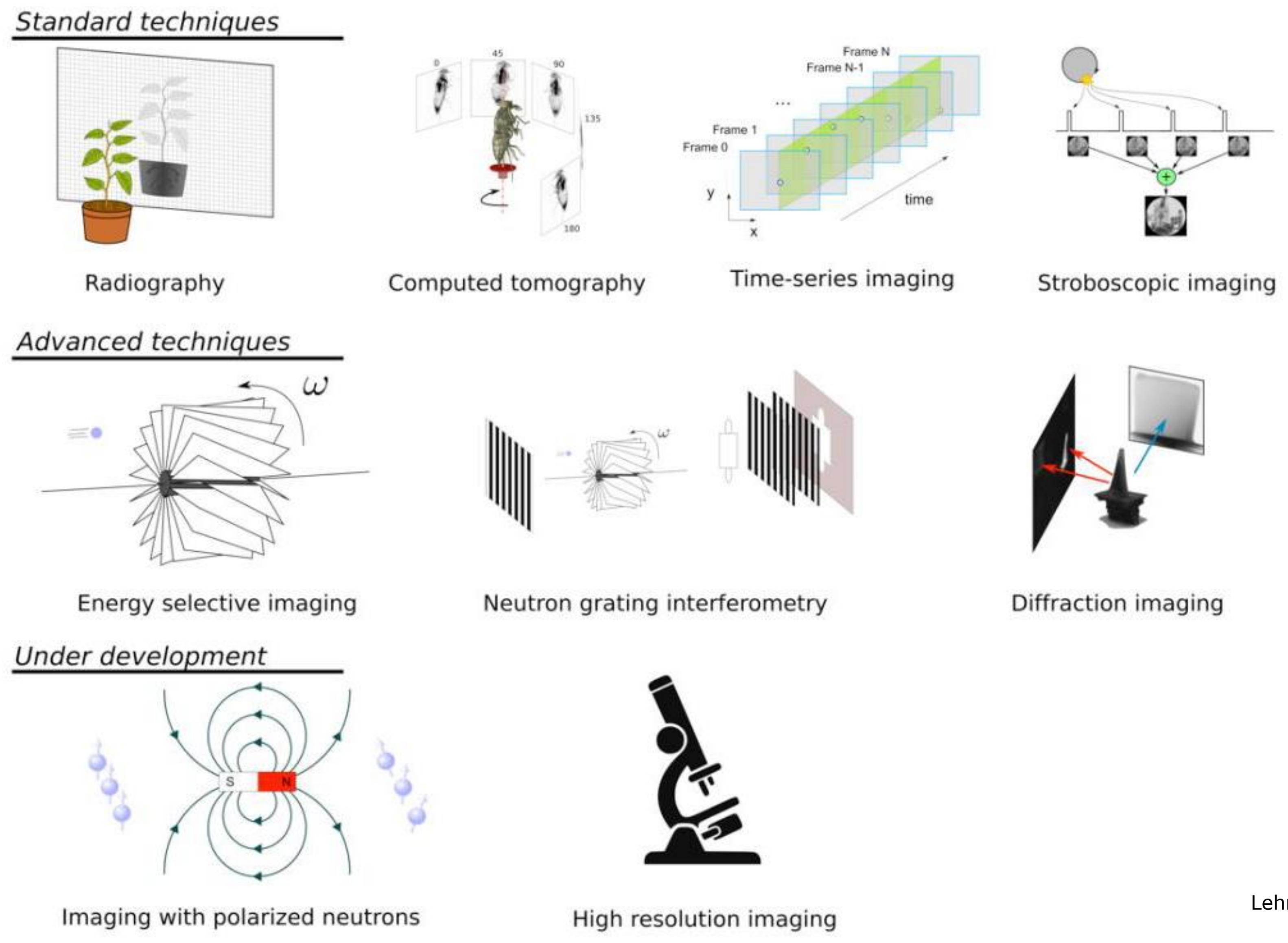

Lehmann, E. et al. (2017). *Phys. Proc.* **88**, 5.

Radiography

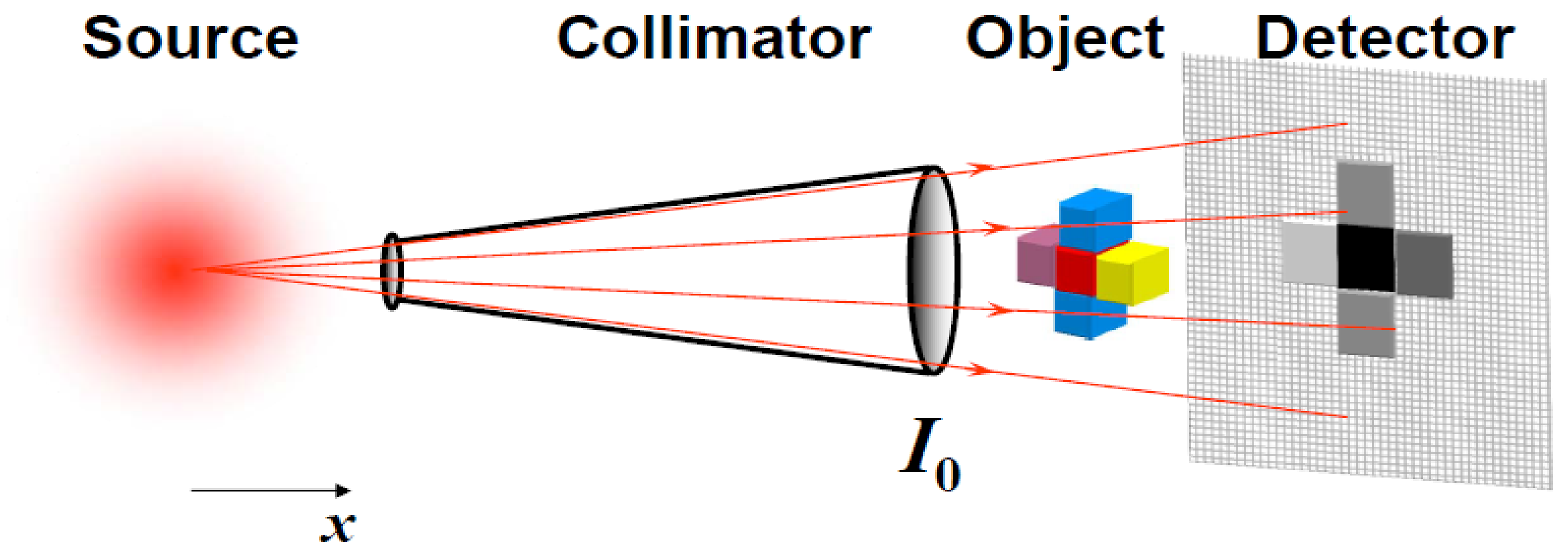

Beer-Lambert law: $\sim I_0 e^{-\int \mu(x)dx}$

x – propagation direction

I_0 – primary beam

$\mu(x)$ – attenuation coefficient

$\mu_{total} = \mu_a + \mu_s$

Strobl, M. et al. (2009). *J. Phys. D. Appl. Phys.* **42**, 243001.

Neutron imaging

Source Collimator Object Detector

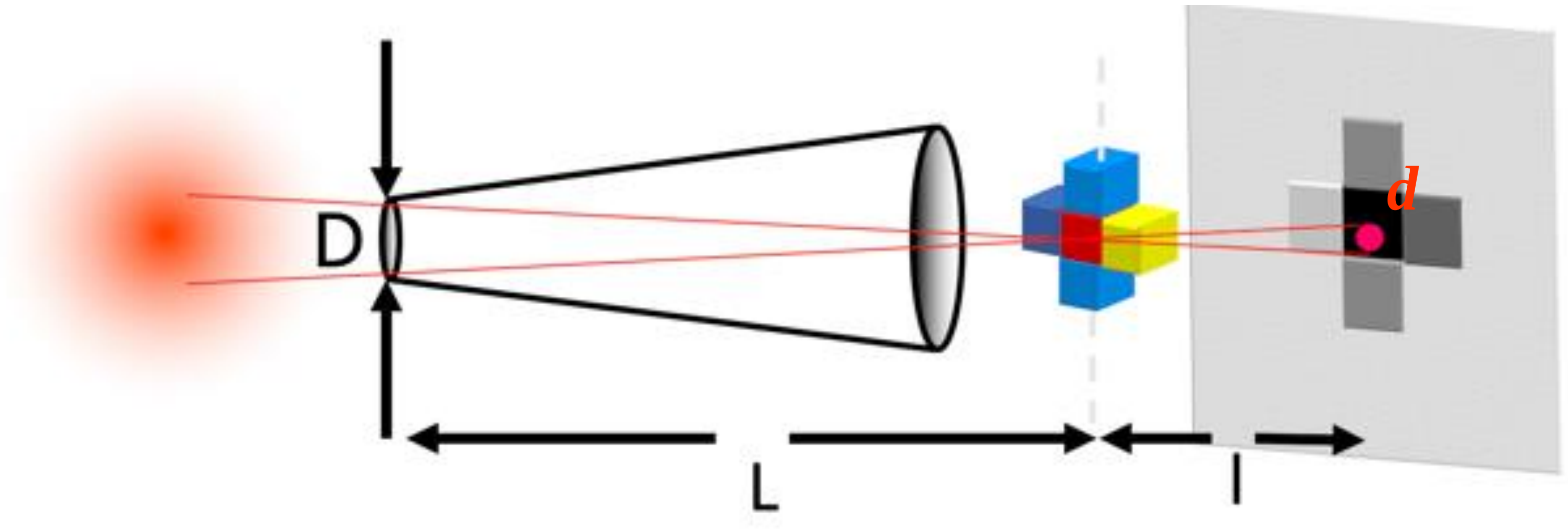

D – Collimator aperture, pinhole

L – Distance Collimator-Object

l – Distance Object-Detector

Spatial resolution

$$d = \frac{l}{L/D}$$

Total neutron scattering cross section

Beer-Lambert law:

$$\sim I_0 e^{-\int \mu(x) dx}$$

I_0 – primary beam

$\mu(x)$ – attenuation coefficient

$$\mu_{total} = \mu_a + \mu_s$$

Strobl, M. et al. (2009). *J. Phys. D. Appl. Phys.* **42**, 243001.

Setup: ICON @ Paul Scherrer Institute

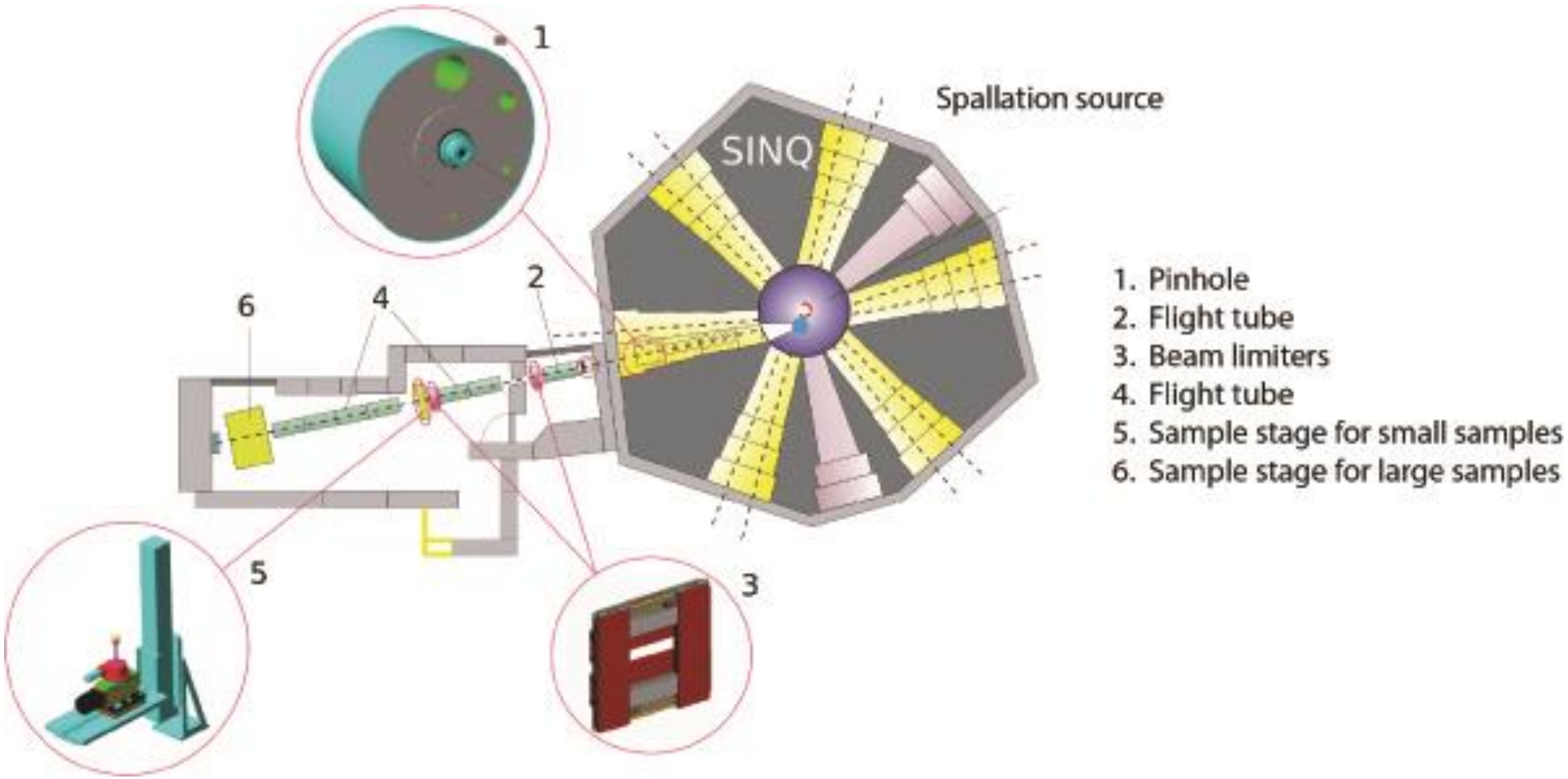

Detectors

Charged Coupled Device

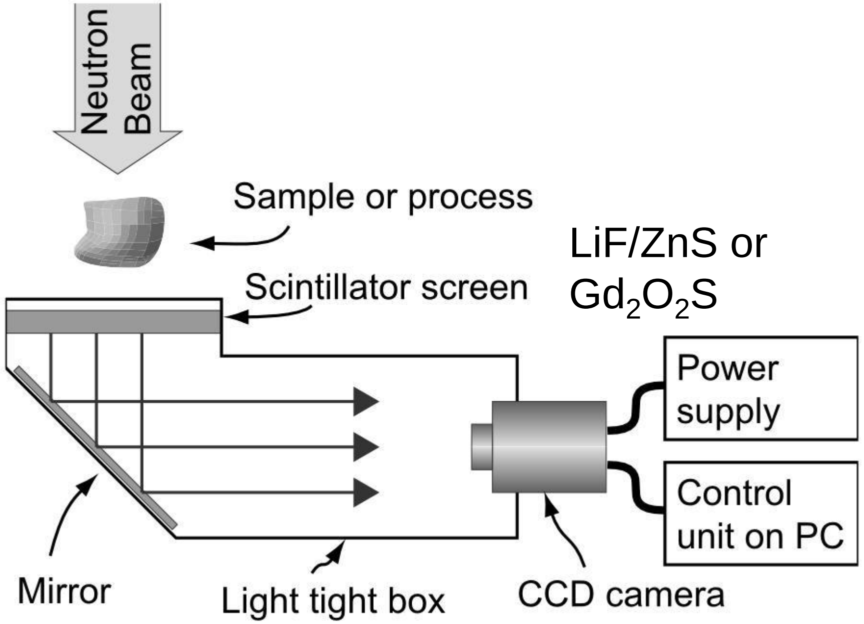

LiF/ZnS or Gd_2O_2S

Multi Channel Plate

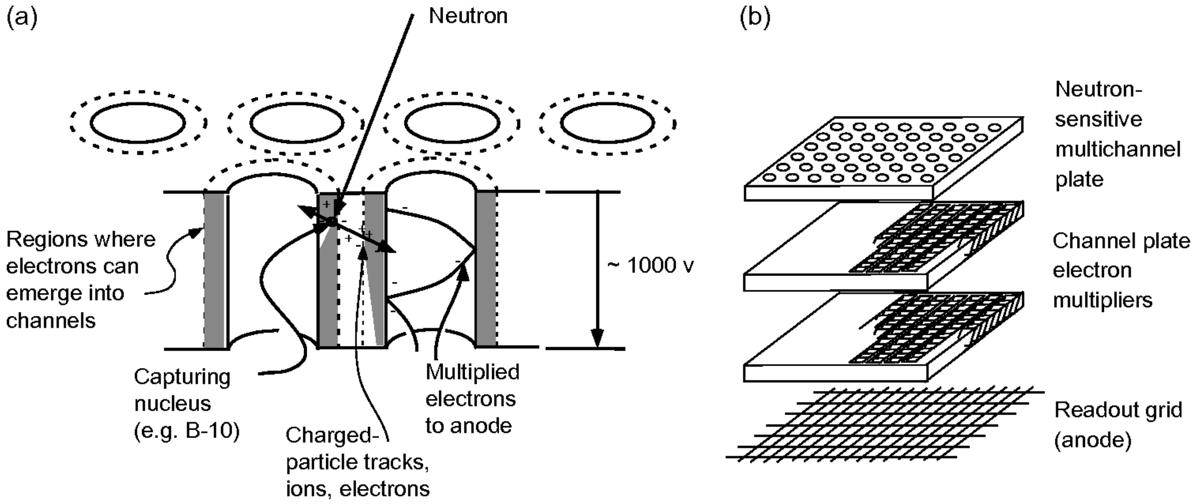

http://www.novascientific.com/technology/

Field of view: 0.5x0.5 m^2 to 5x5 mm^2
Pixel size: 500x500 μm^2 to 1.5x1.5 μm^2

Spatial resolution - Siemens star

32.9 μm

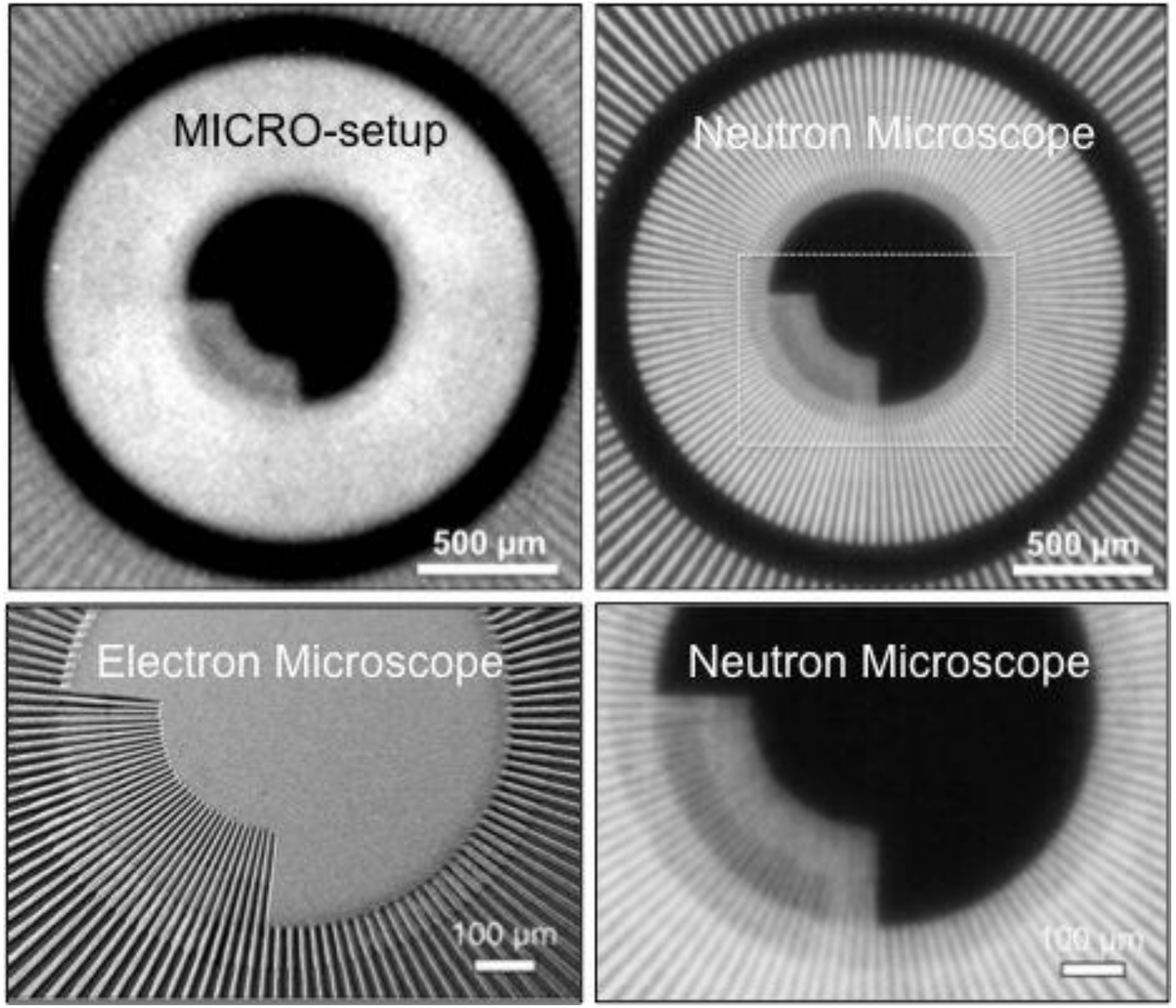

7.6 μm

Trtik, P. et al. (2015). *Physics Procedia.* **69**, 169.

Neutron microscope with neutron optics

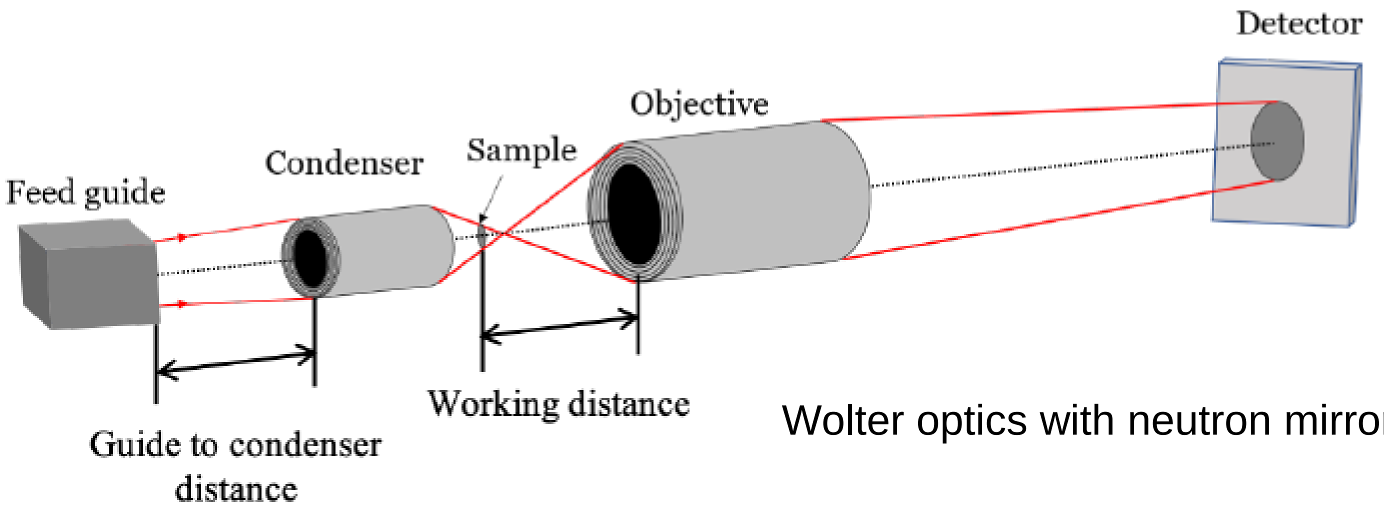

Wolter optics with neutron mirrors

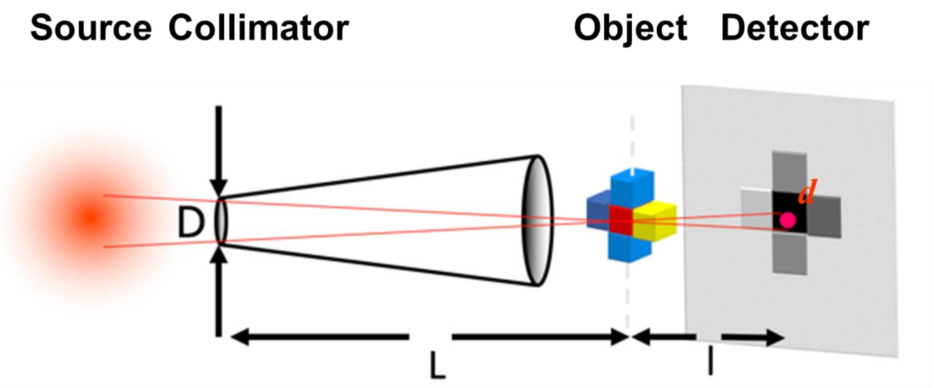

D – Collimator aperture, pinhole

L – Distance Collimator-Object

l – Distance Object-Detector

$$d = \frac{l}{L/D}$$

M. Abir et al. (2020). *Journal of Imaging.* **6**, 100.

Principle for data acquisition in imaging experiment

1. Raw image, I_θ
2. Dark field image (no beam), correct for dark-current in detector system, *DF*
3. Flat-field image (open beam), correct for inhomogeneities in beam-profile and in detector screen, *FF*
4. Image, T_θ

$$T_\theta = \frac{I_\theta - DF}{FF - DF}$$

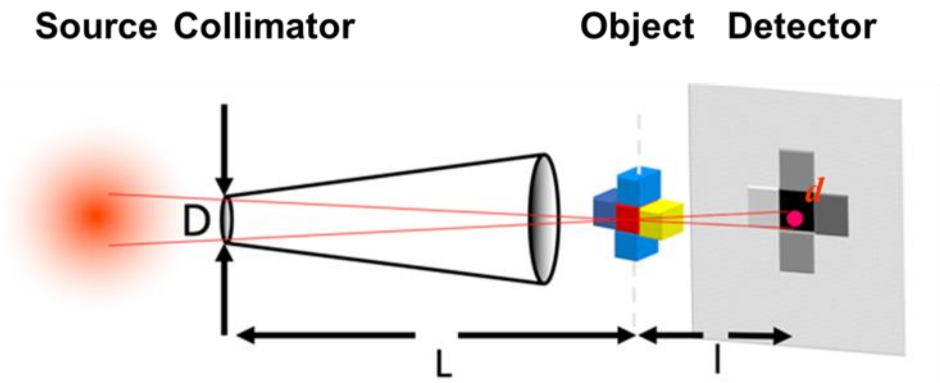

Cases: water uptake in plants

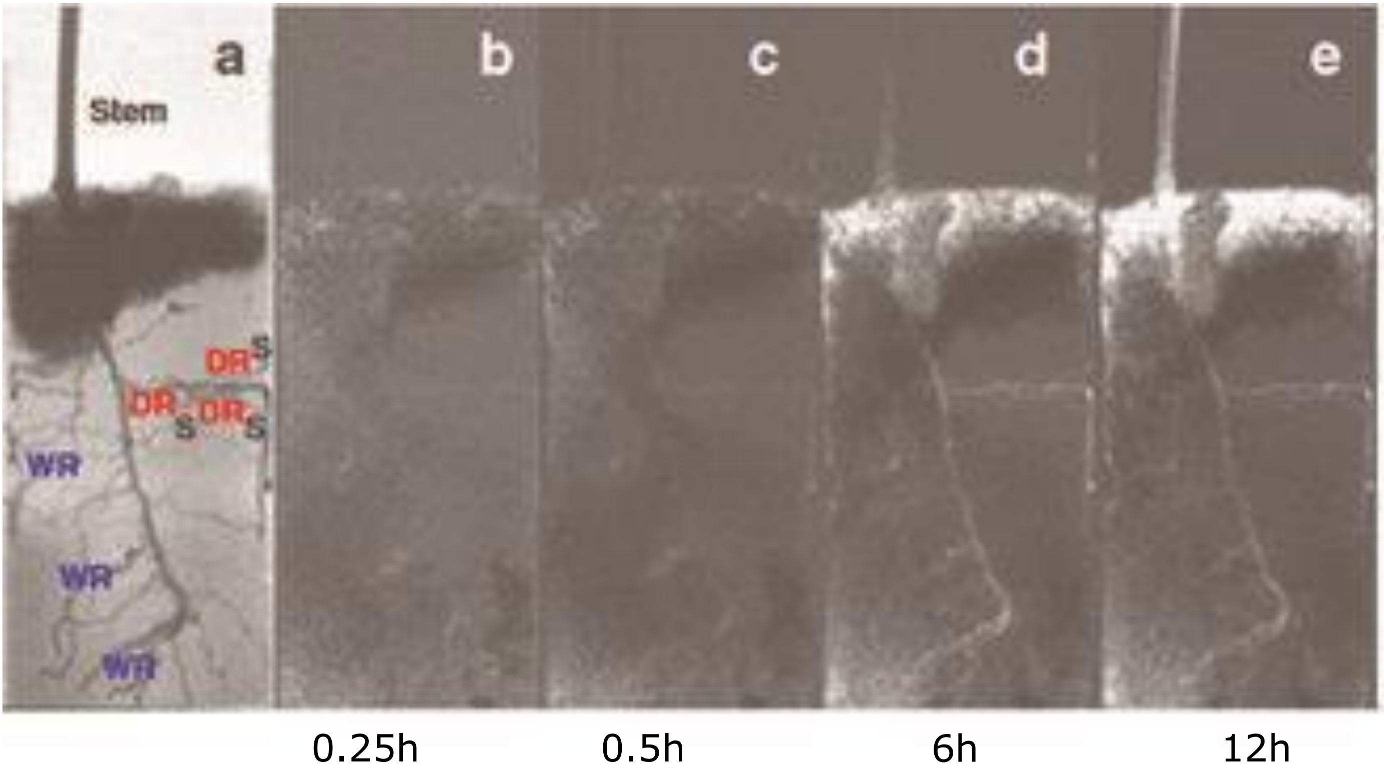

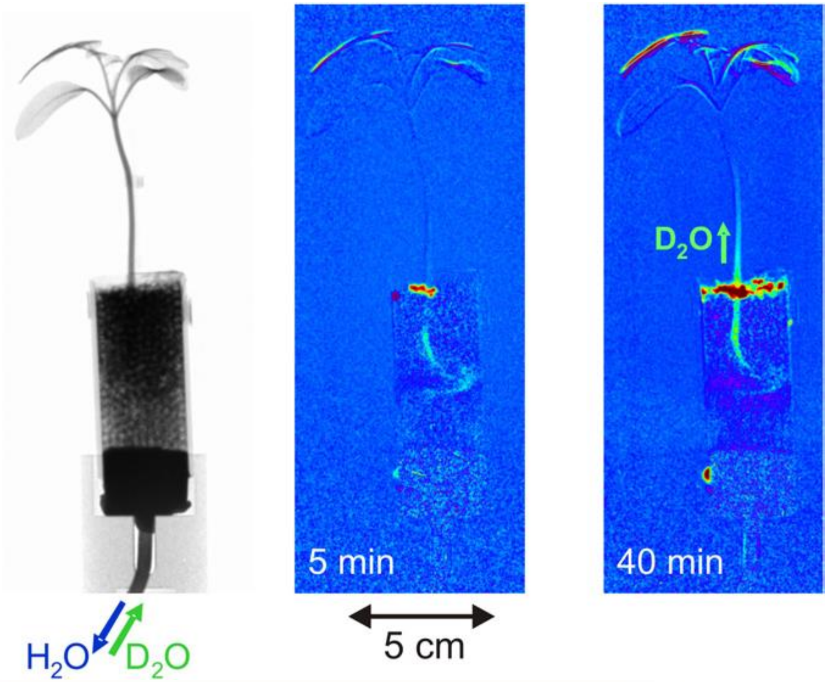

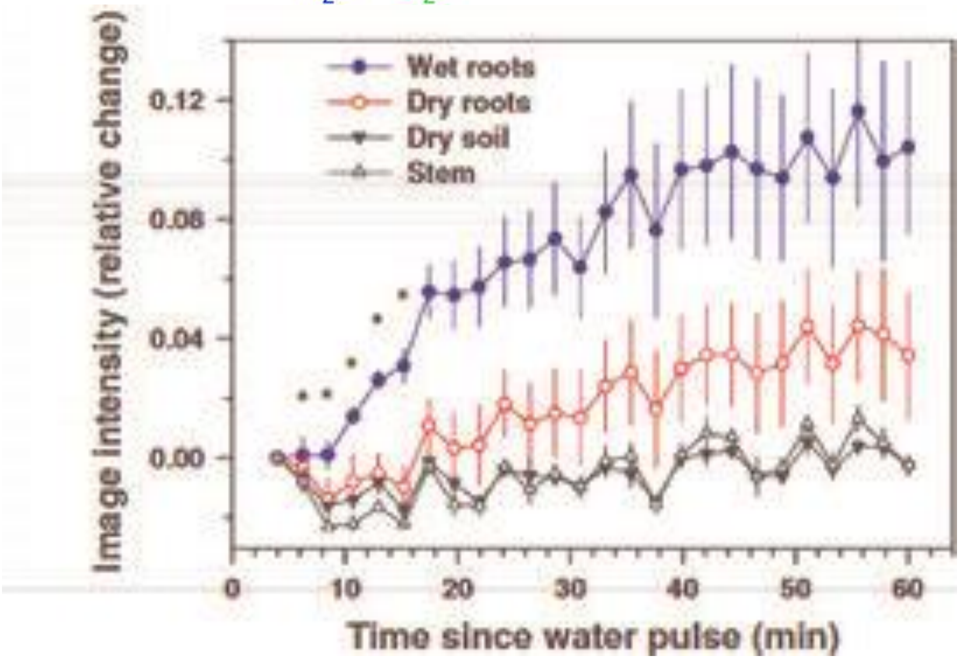

Strobl, M. et al. (2009). *J. Phys. D. Appl. Phys.* **42**, 243001.

Cases: Cultural heritage

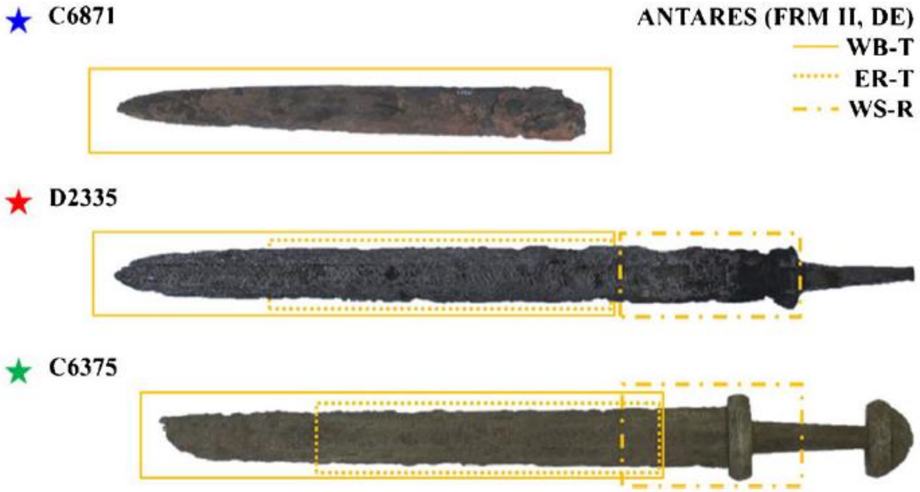

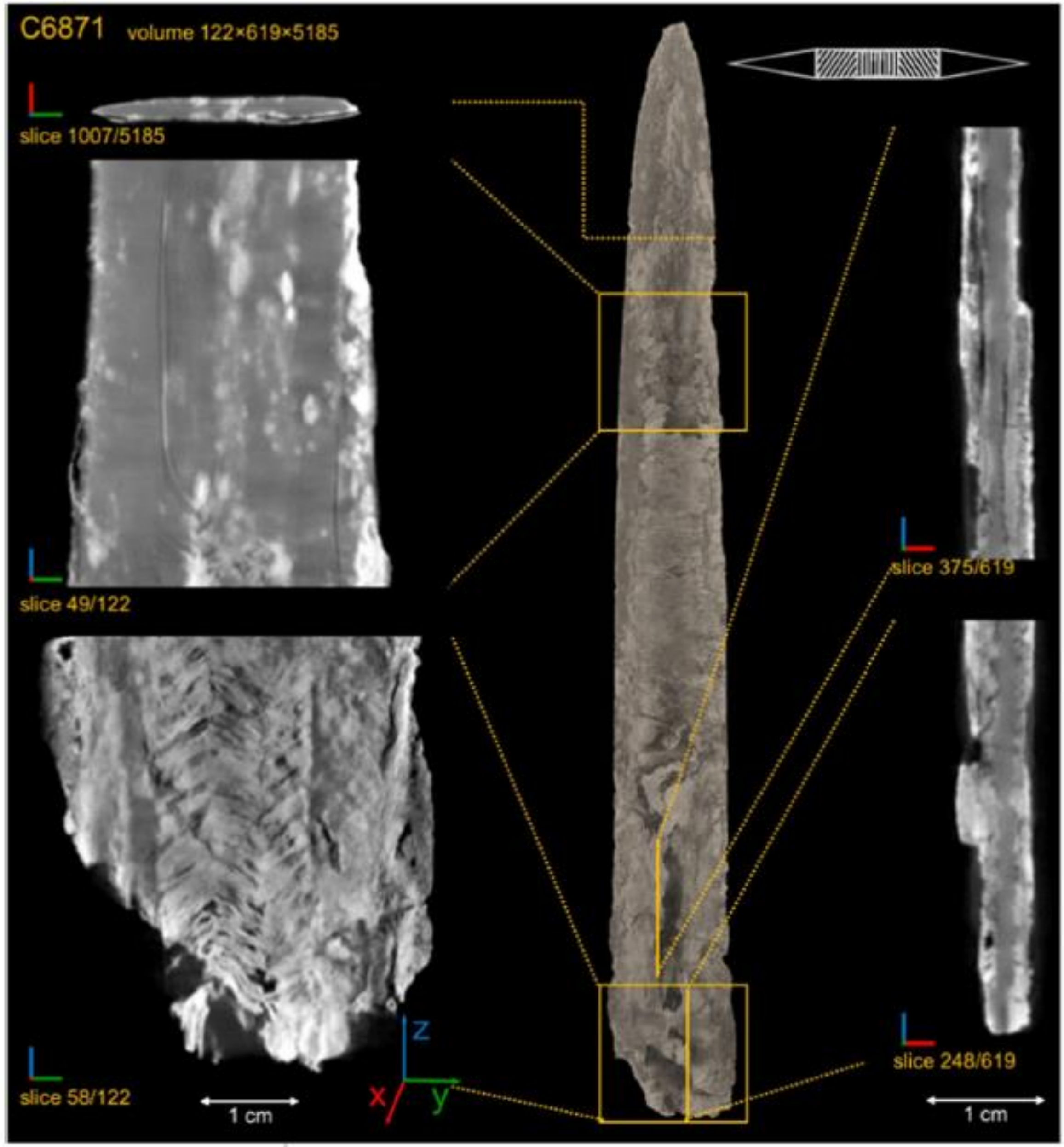

A. Fedrigo et al, *Archaeol Anthropol Sci (2018)* **10**,1249–1263

Tomography

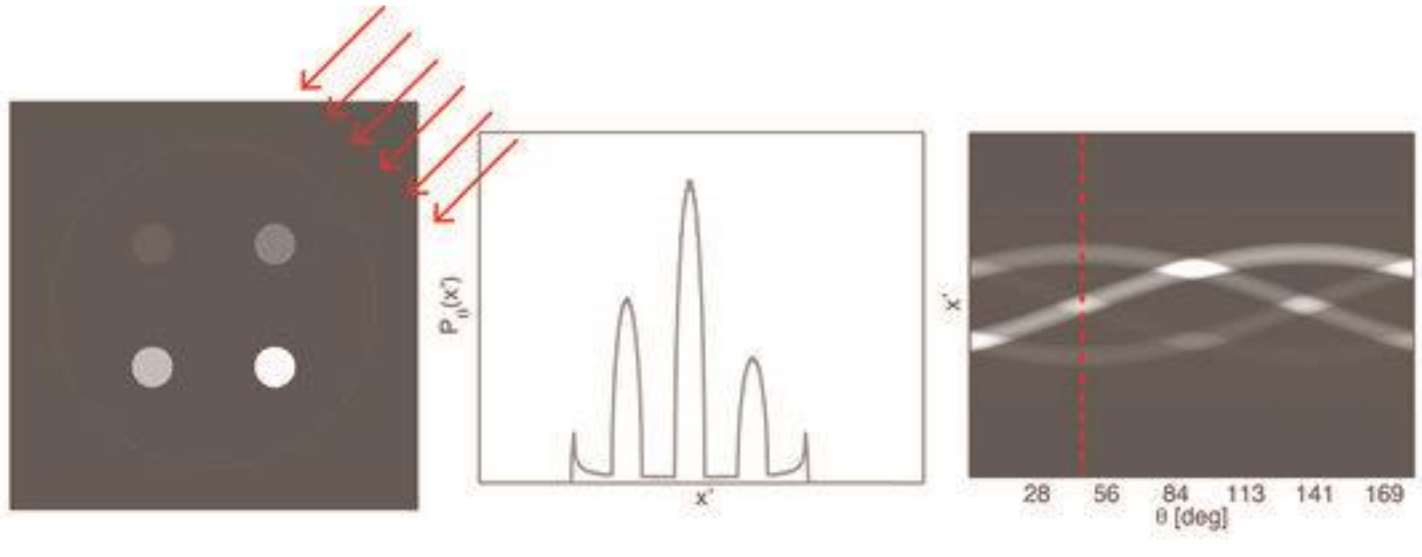

2D sample

Projection image T_θ

Sinogram

no. of projections n with resolution d of object with size R

$$n = \frac{\pi}{2}\frac{R}{d}$$

Tomographic reconstruction – Radon transform

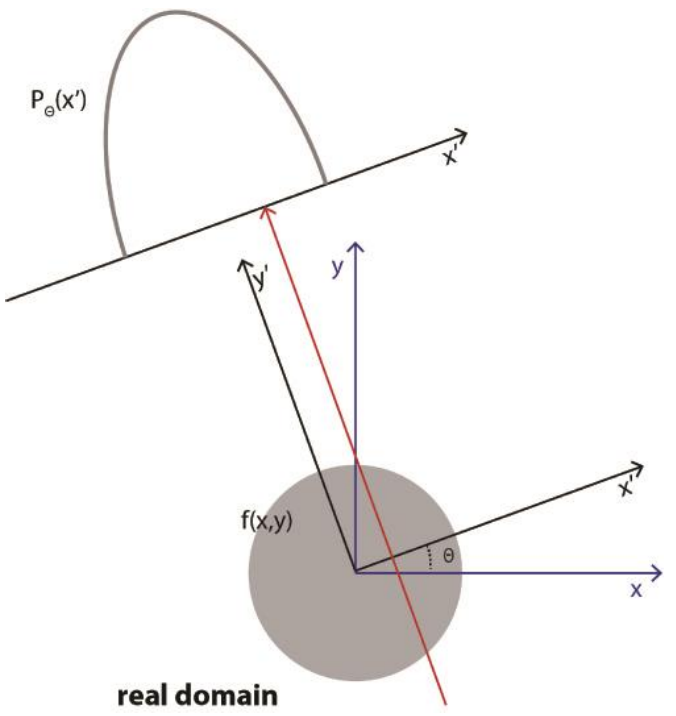

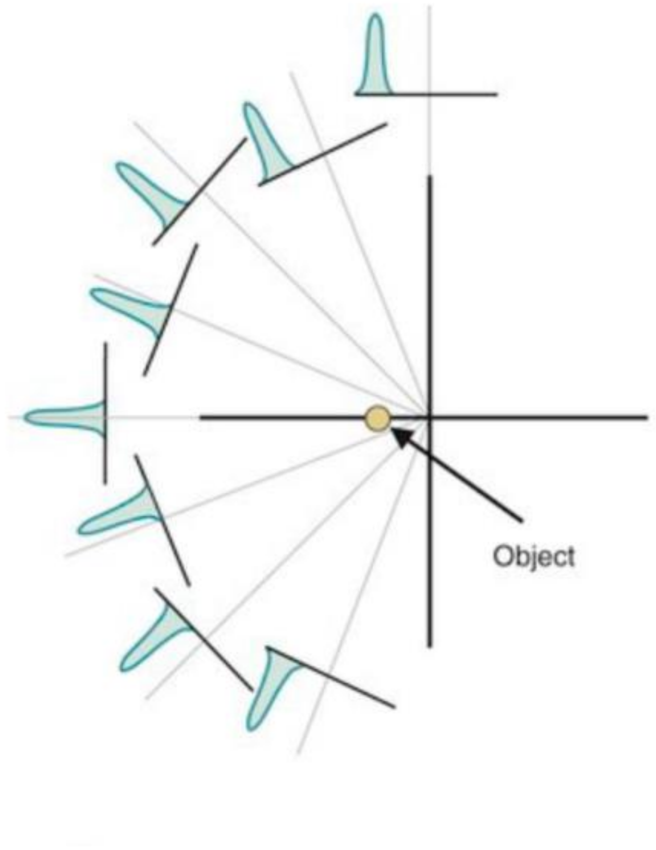

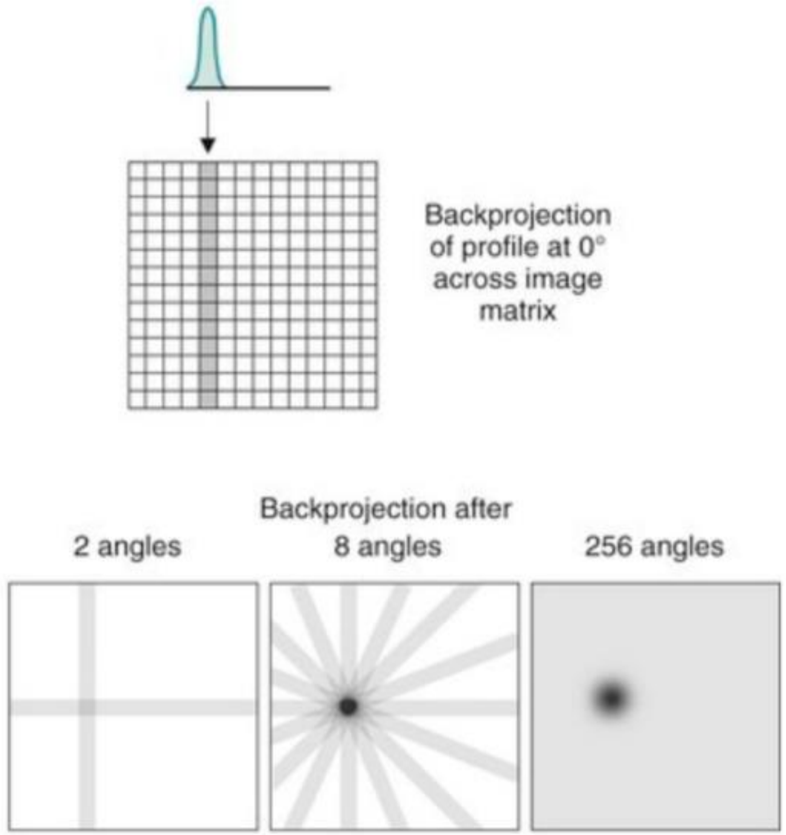

Principle for tomographic reconstruction

1. Collect projections, $P_\theta(x')$, for several angles
2. Calculate the Fourier transform of each projection
3. Apply the Fourier filter to approximate the ideal case
4. Find the inverse Fourier transformation of the filtered projection
5. Sum over all angles to make the reconstruction

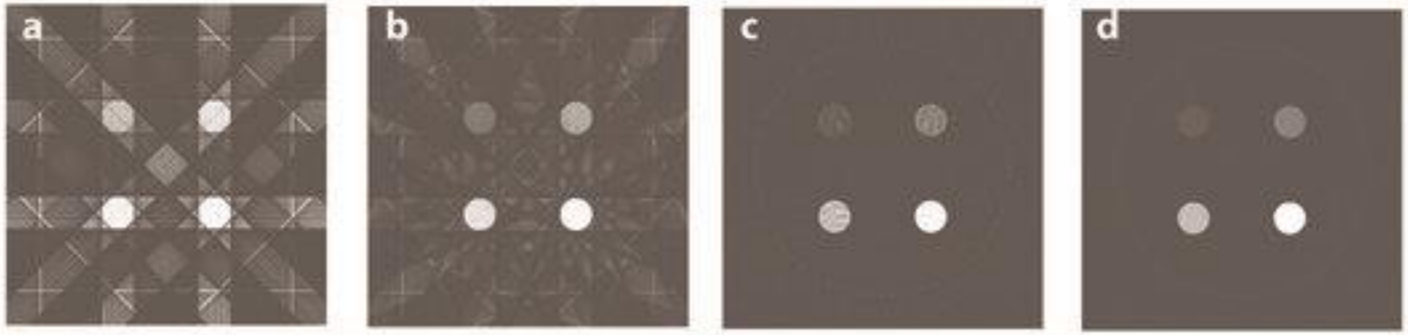

4 projections   8 projections   32 projections   128 projections

Cases:
Soot in particulate filter for diesel engine

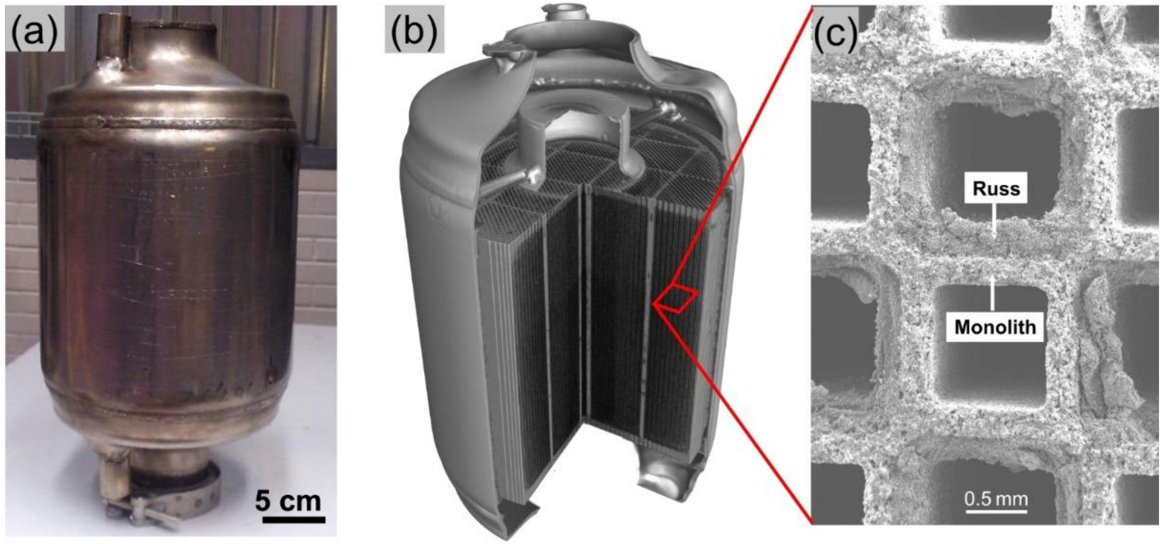

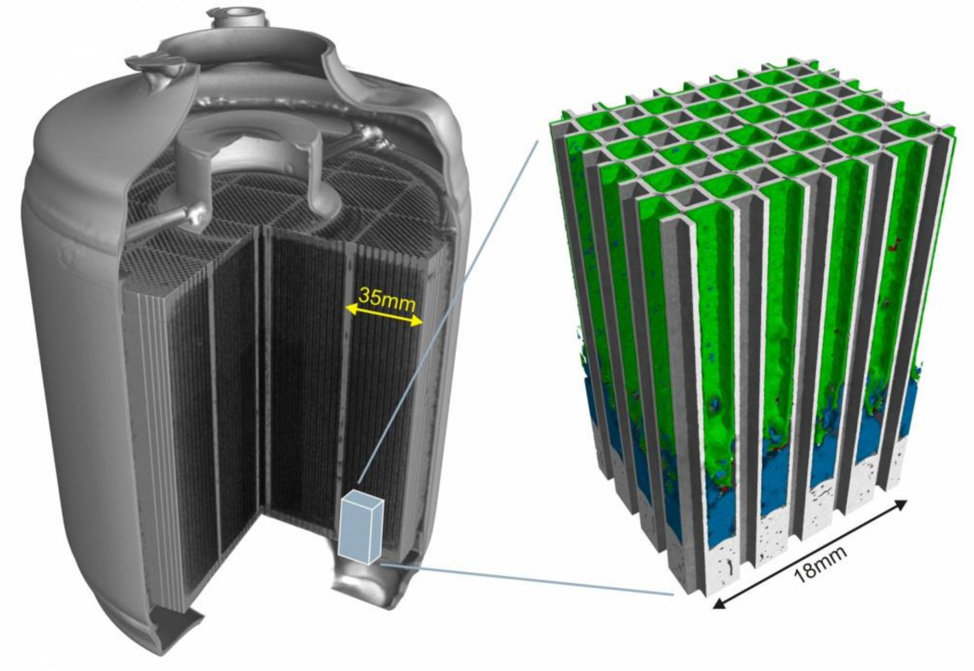

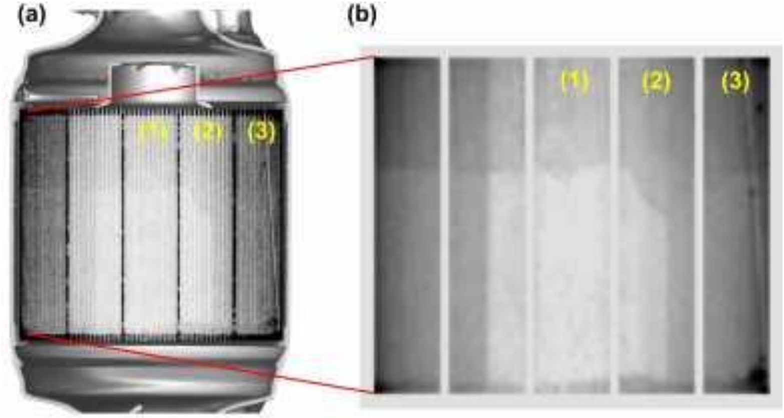

https://www.psi.ch/media/distribution-of-soot-particles-in-particulate-filters-of-diesel-vehicles

Cases: Aging of Li-ion rechargeable battery

NEUTRA@PSI

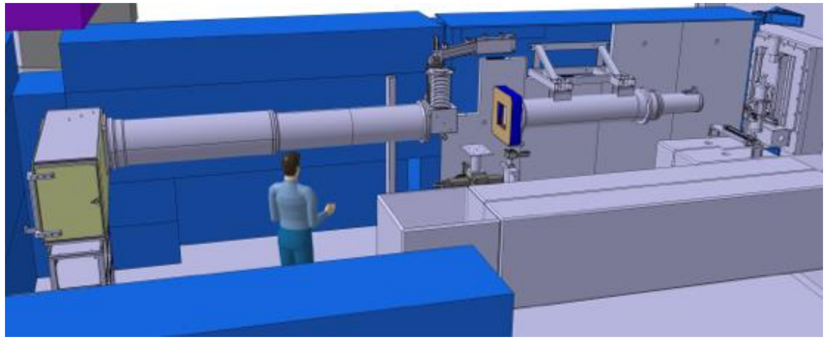

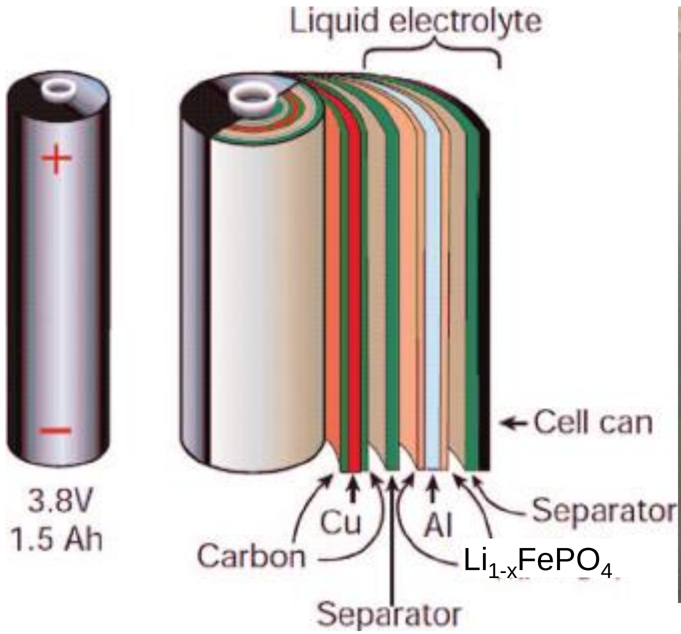

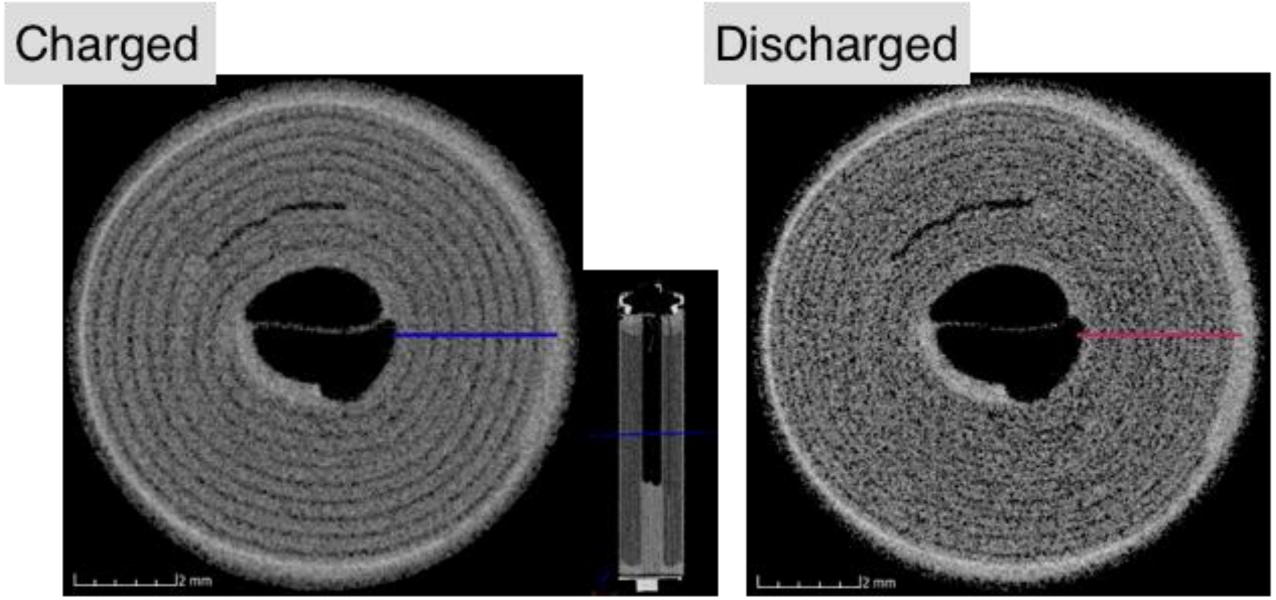

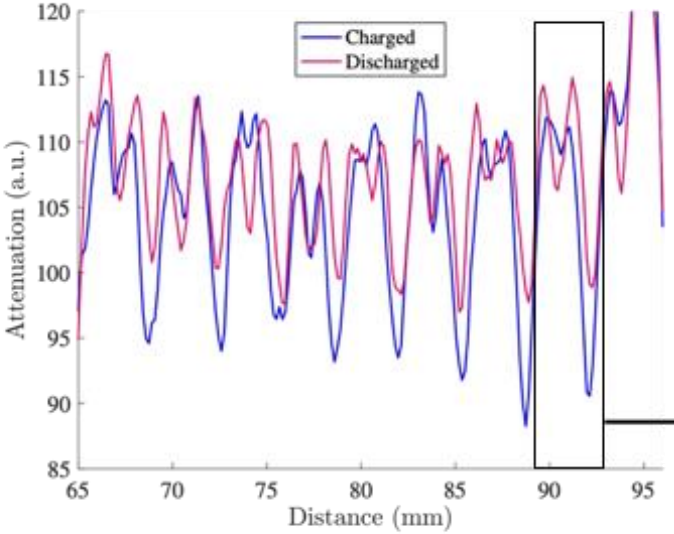

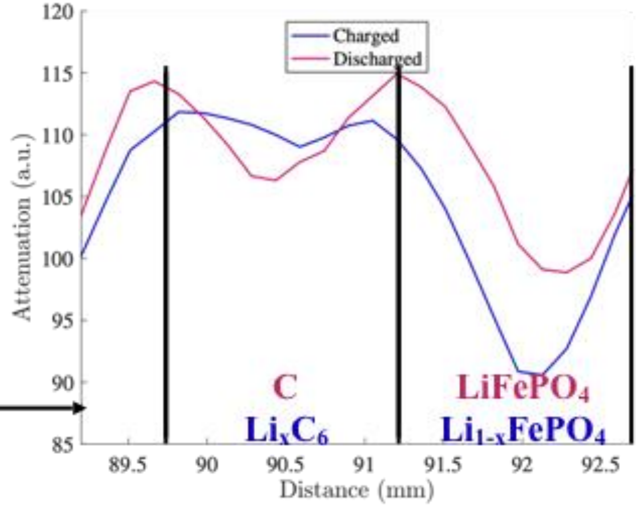

Break – 10 min

clipartpng.com

Energy-resolved neutron imaging
Bragg-edge imaging

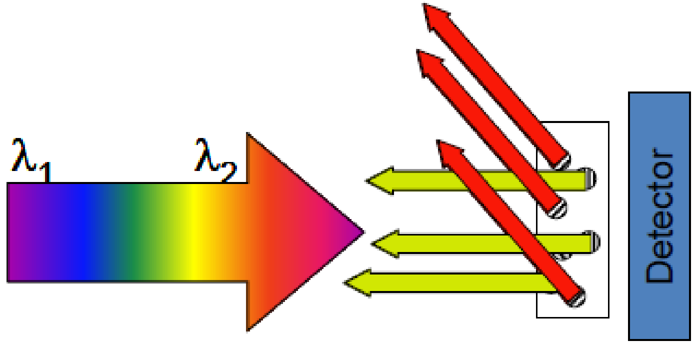

Bragg's law:

$2d_{hkl}\sin\theta = \lambda$

$2d_{hkl}\sin 90^\circ = \lambda$

$2d_{hkl}\sin\theta < \lambda$

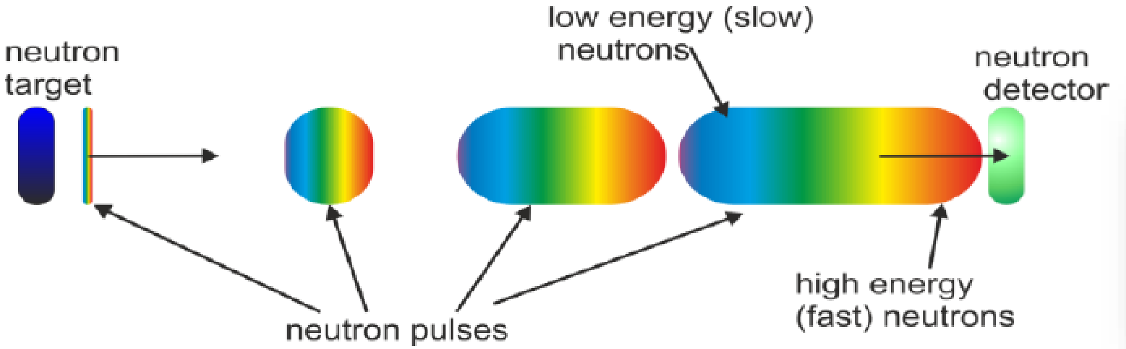

Total neutron cross section for different polycrystalline materials

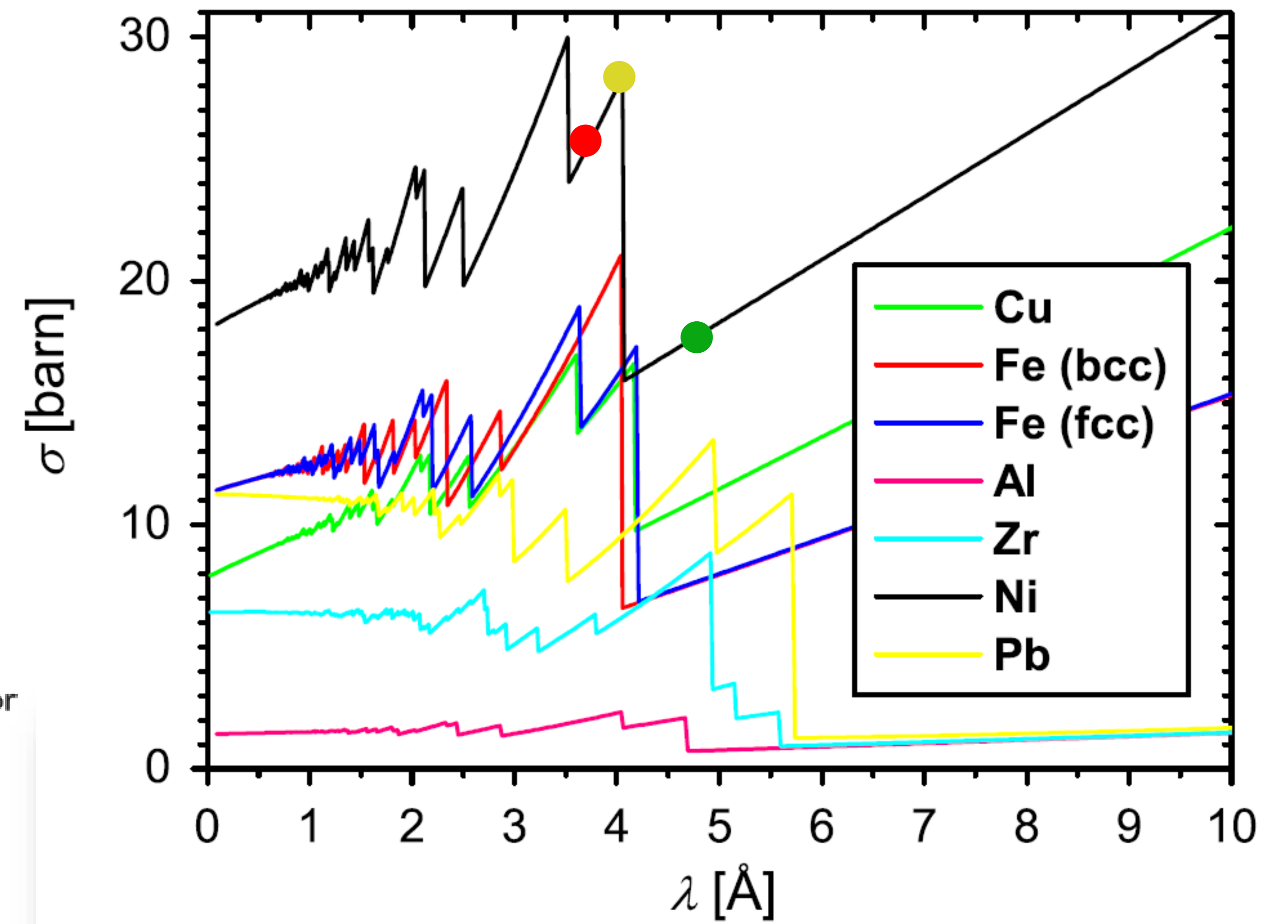

Josic, L. et al (2011). *Nucl. Instruments Methods Phys. Res.* **651**, 166.

Energy-resolved neutron imaging
Case: welding of steel

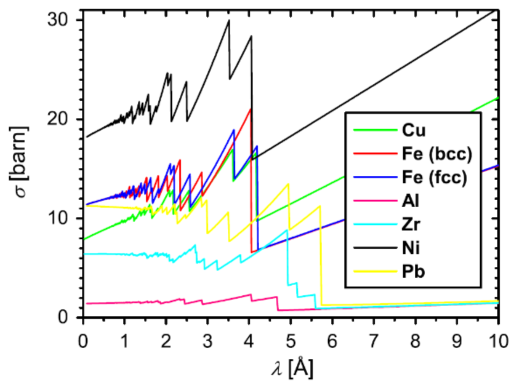

3.4 Å

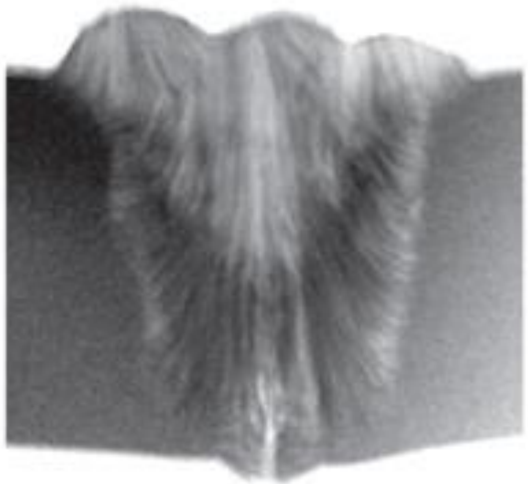

4.0 Å

4.4 Å

Solid Oxide Electrochemical Cell (SOFC/SOEC)

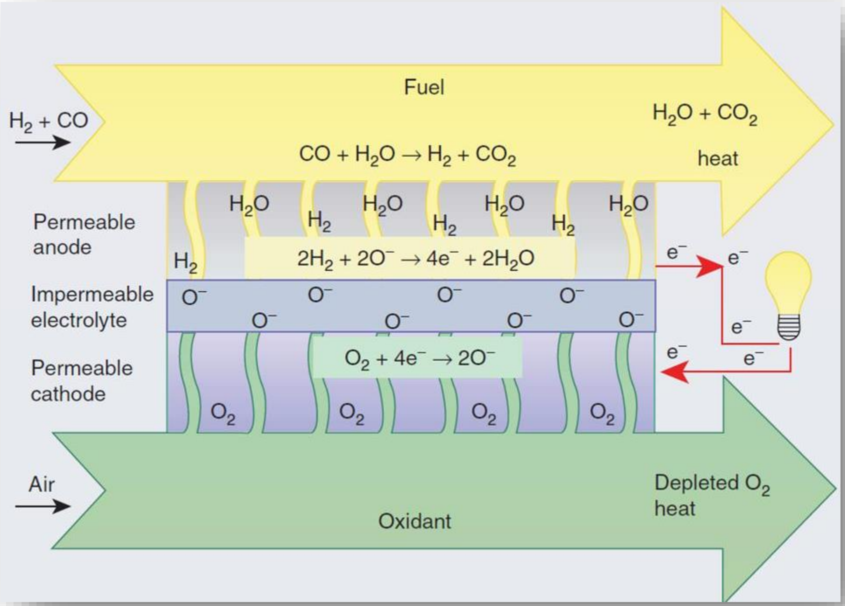

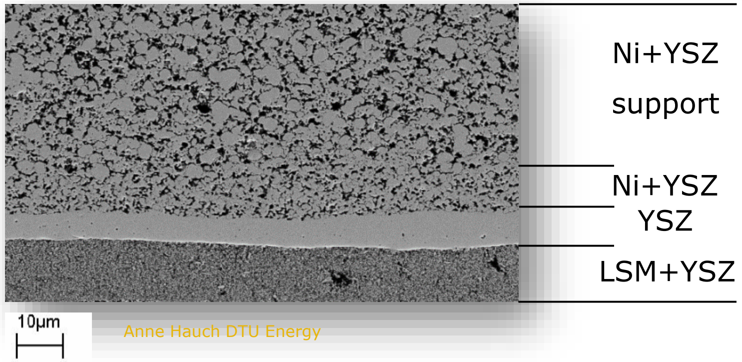

Anne Hauch DTU Energy

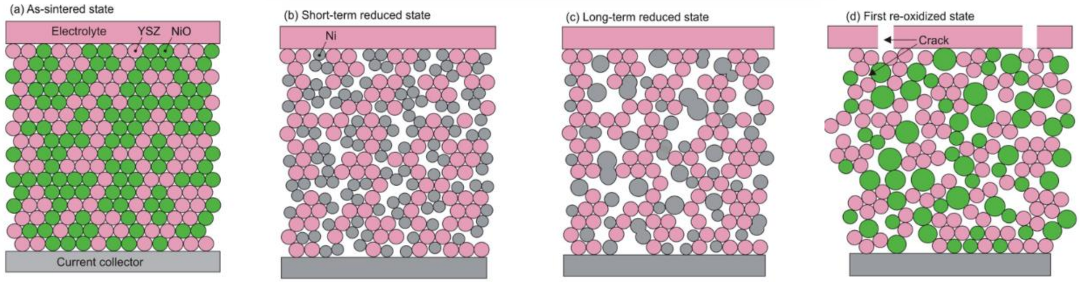

Cases: In-situ Bragg-edge imaging linking strain and NiO reduction in Solid Oxide Fuel/ Electrolysis Cell electrodes

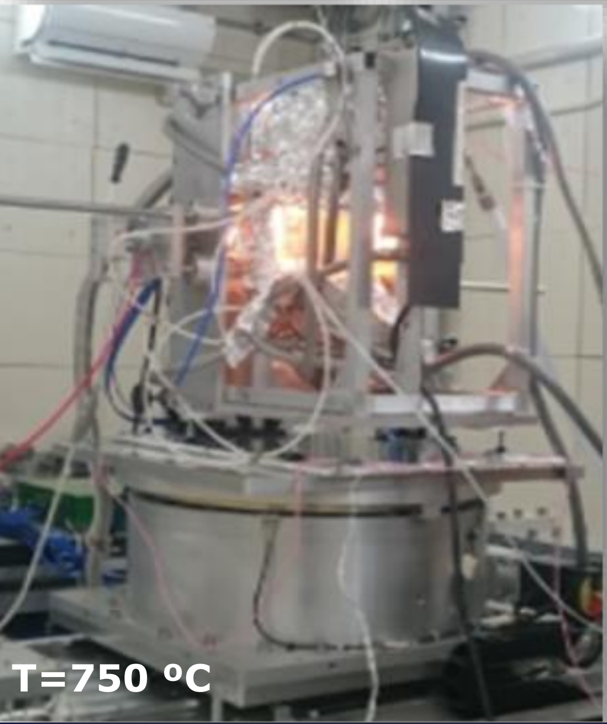

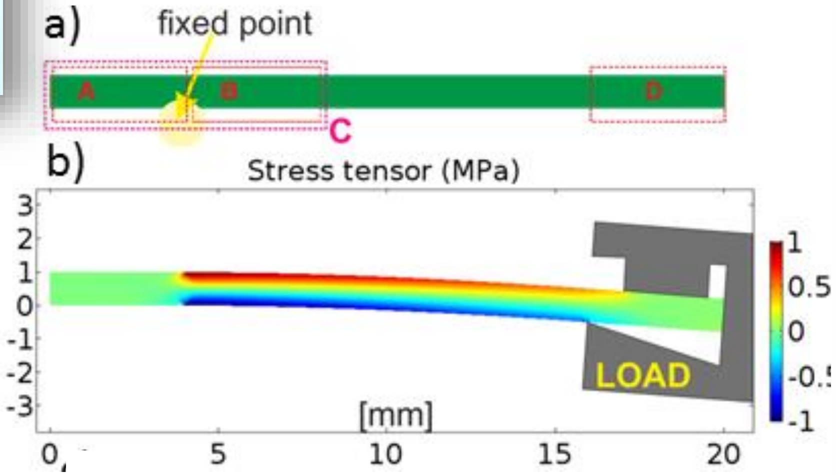

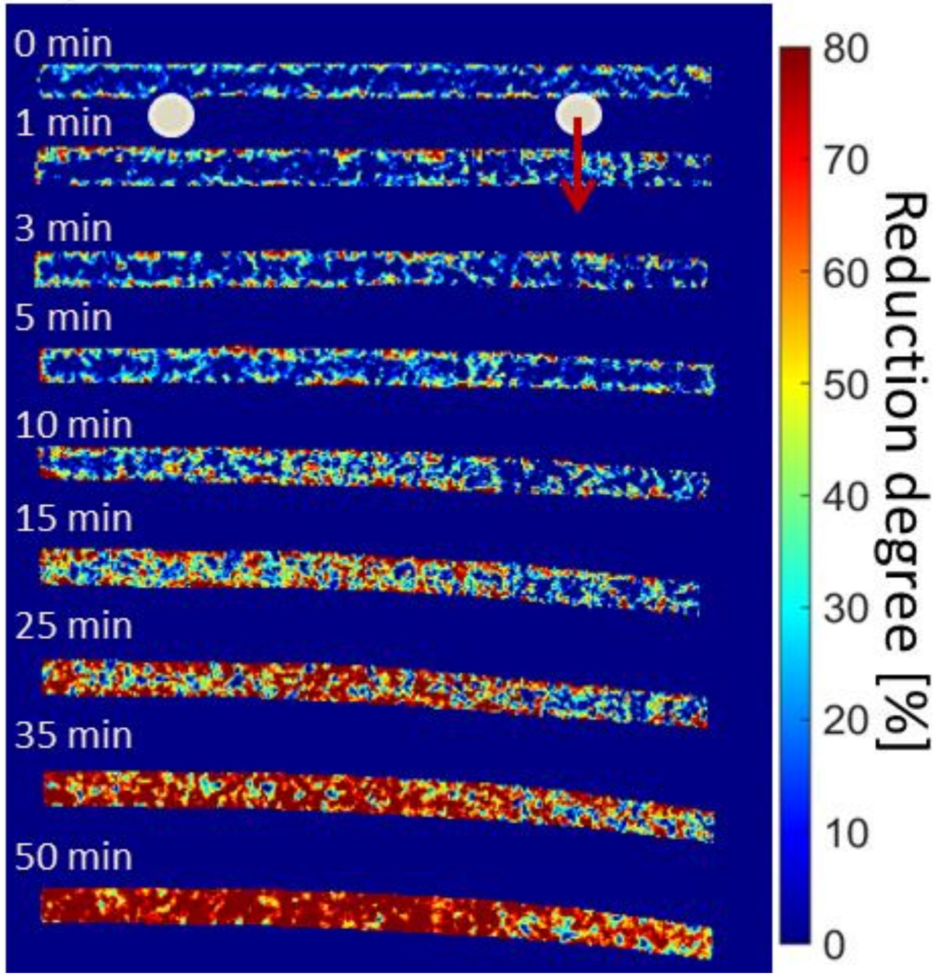

M. Makowska et al, J.Appl.Cryst. **48**, *401(2015)*

M. Makowska et al, J. Appl. Cryst. **49**, *1674 (2016)*

Neutron Bragg-edge tomography of crack evolution after 5x red-ox cycling

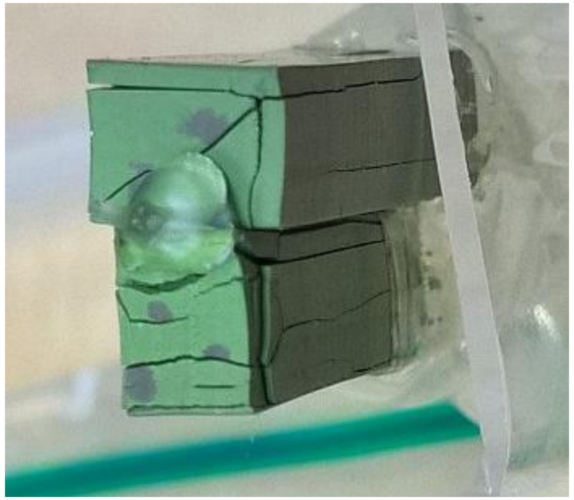

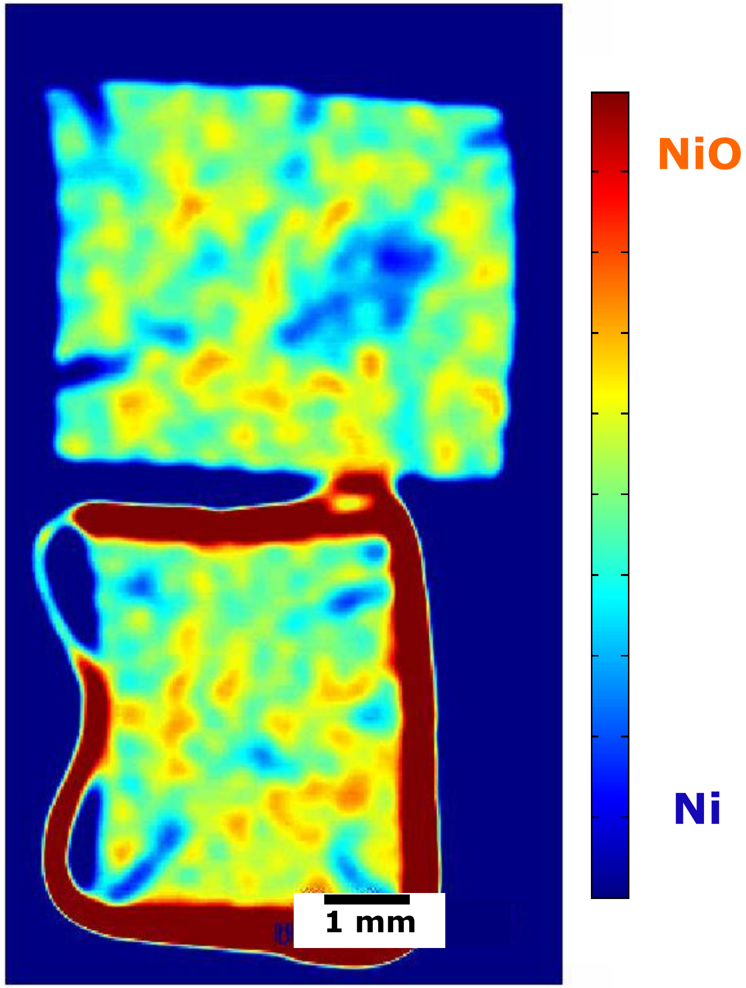

M. Makowska et al, Physica B: Cond. Matter 551, 24-28 (2018)

Degradation of batteries - a multi-scale challenge

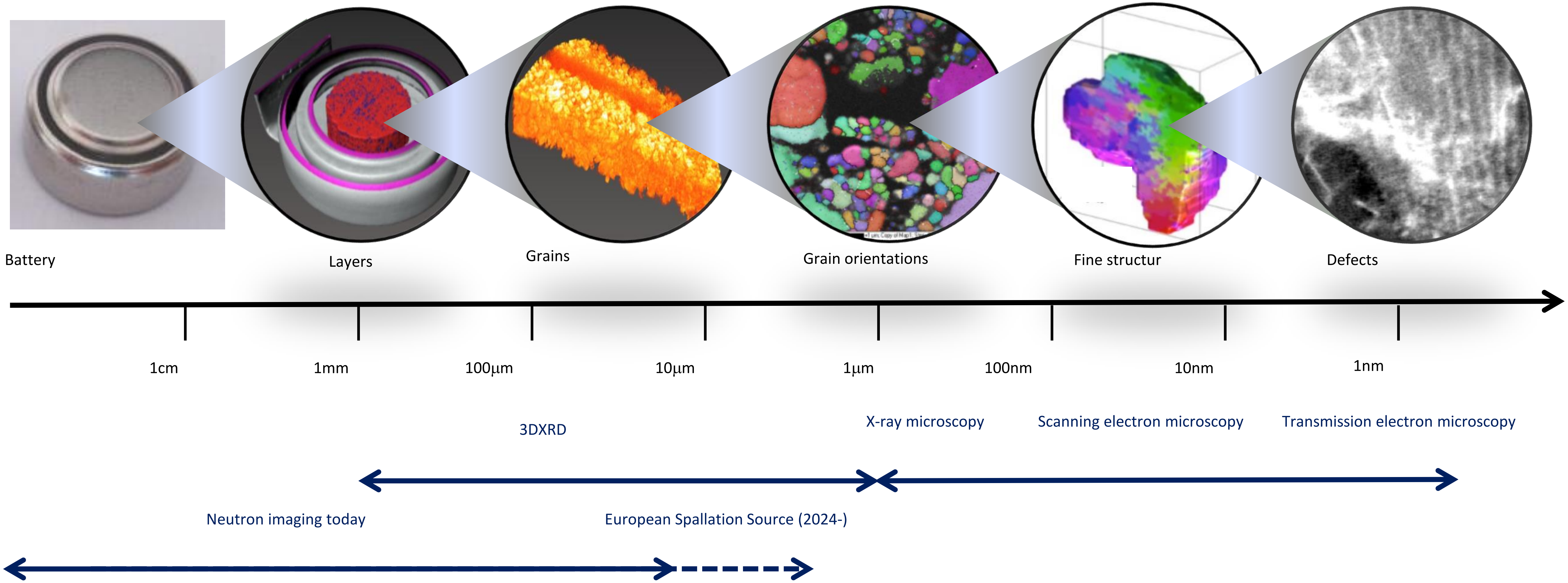

Multi-modal neutron 3D imaging and diffraction

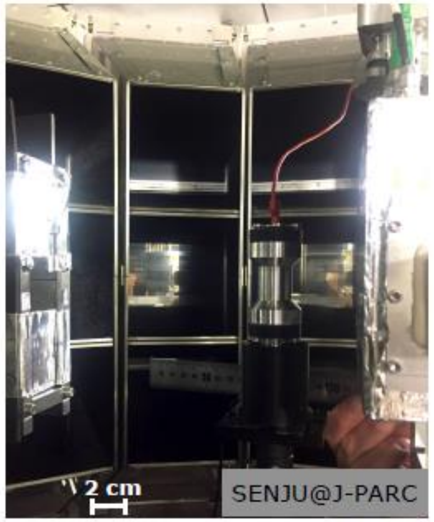

Imaging detector:
- 55x55 μm² & 512x512 pixel array
- 1774 wavelength resolved images
- Adapted range: 2.0 Å - 6.4 Å
- 20.48 μs temporal binning

Diffraction detector:
- 256x256 mm² & 64x64 pixels
- 90° detector range: 1.7 Å - 4.4 Å

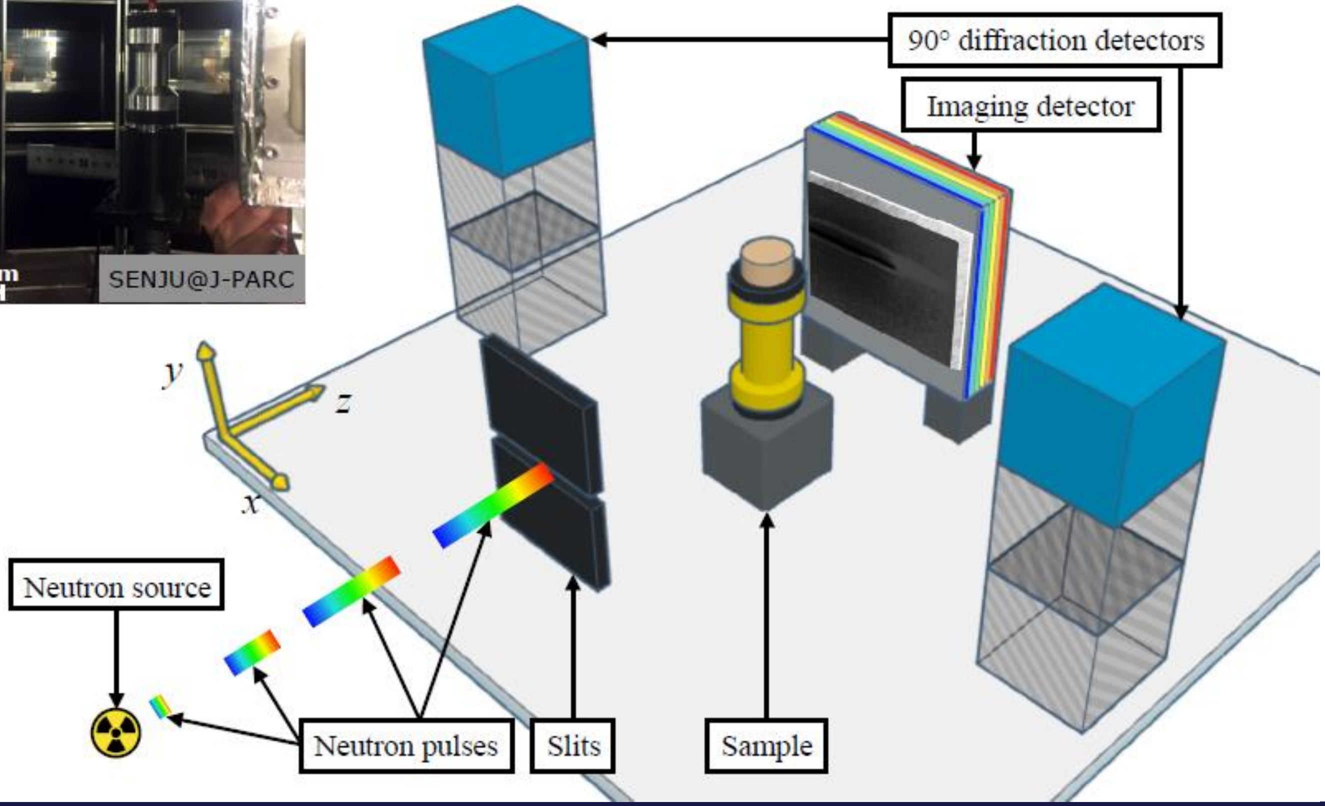

- ➢ Mapping phase, shape, orientation and position of individual detectable grains
- ➢ Strain tensor determination for individual grains -> 3D strain tensor field

Charge-discharge of Li-ion battery – the electrodes

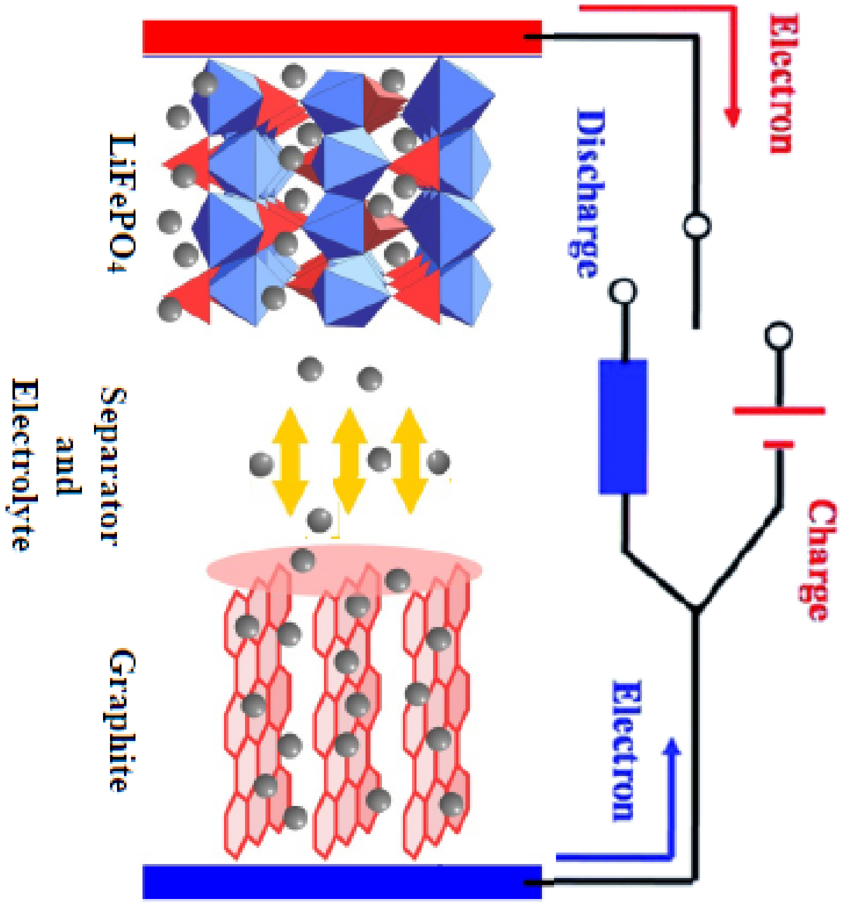

Crystallographic phase changes: $Li_xC_y \underset{\text{lithiation}}{\overset{\text{delithiation}}{\rightleftharpoons}} xLi^+ + xe^- + yC$

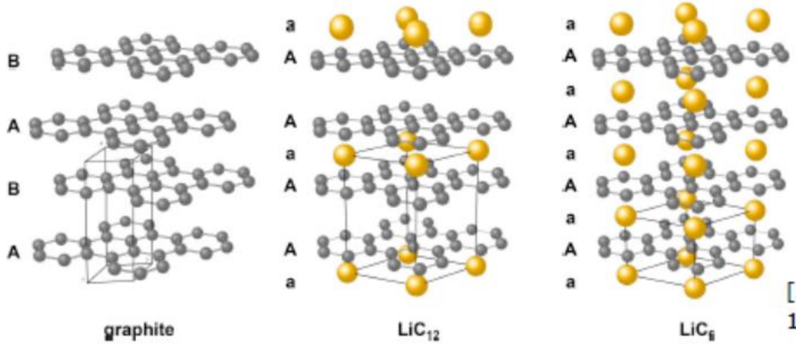

[3] Matsunaga et al., *Carbon*, 142, 513-517 (2019)

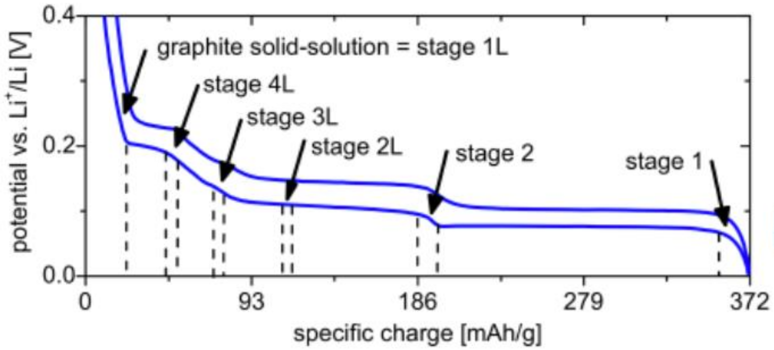

[4] M. Hess, *PhD thesis*, ETH Zürich (2013)

G.-L. Xu et al., *J. Mater. Chem. A*, 2(47), 19941–19962 (2014)

Battery cell for operando neutron tomography

Working Electrode = graphite:carbon PVDF (8:1:1) (740 μm)

Counter Electrode = metallic lithium (760 μm)

Electrolyte: 1 M $LiPF_6$ in EC/DMC: 50/50

Seperator (fiberglas, 50 μm)

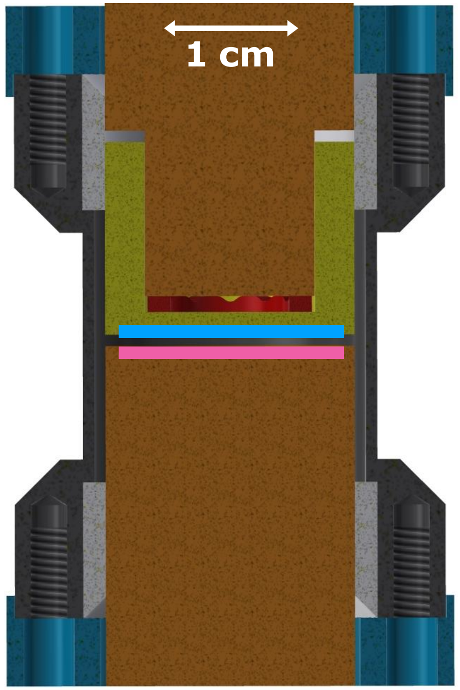

Discharge – charge of model Li-ion battery

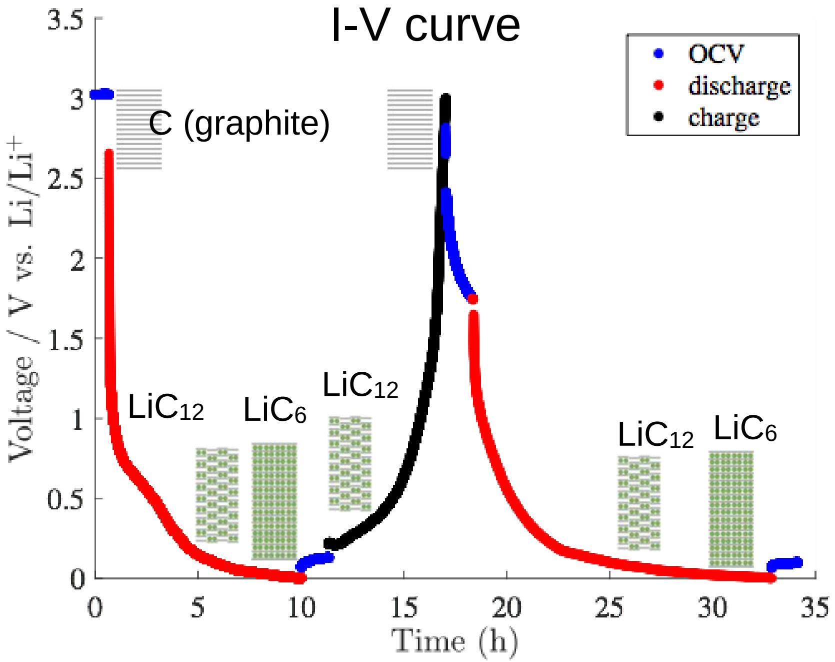

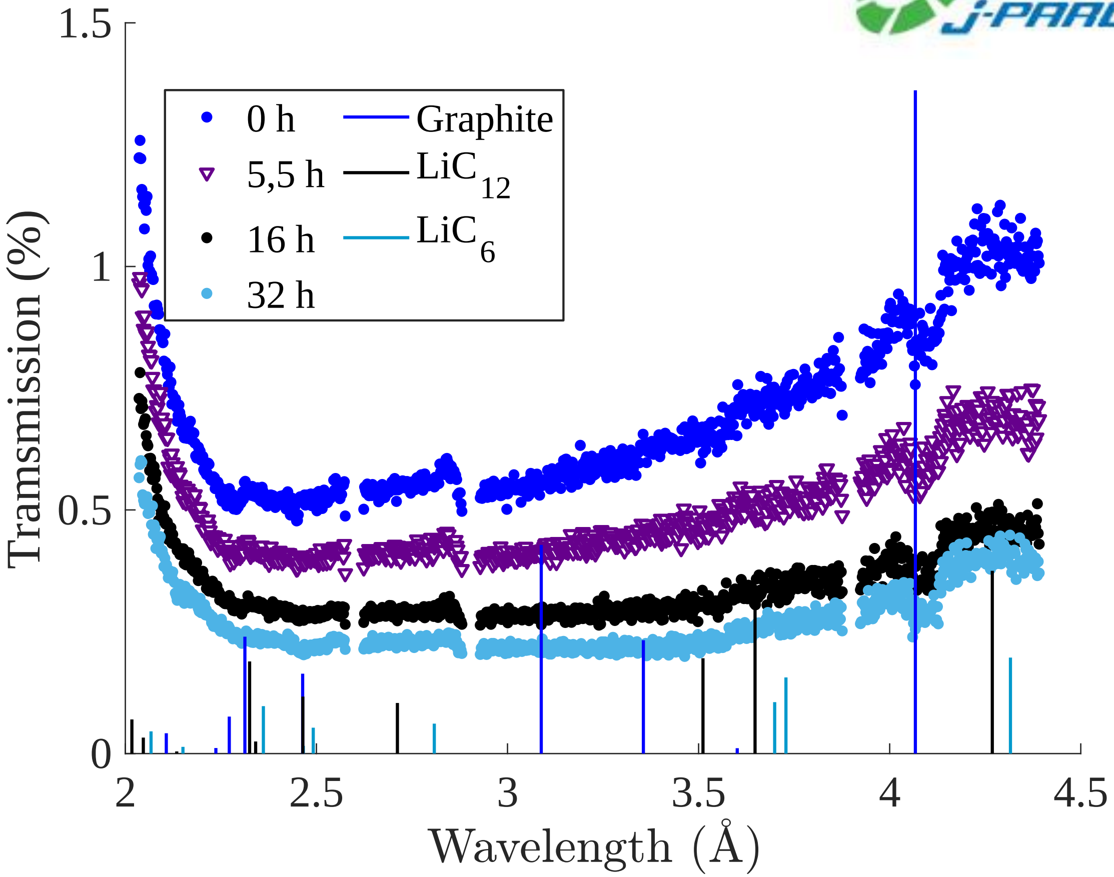

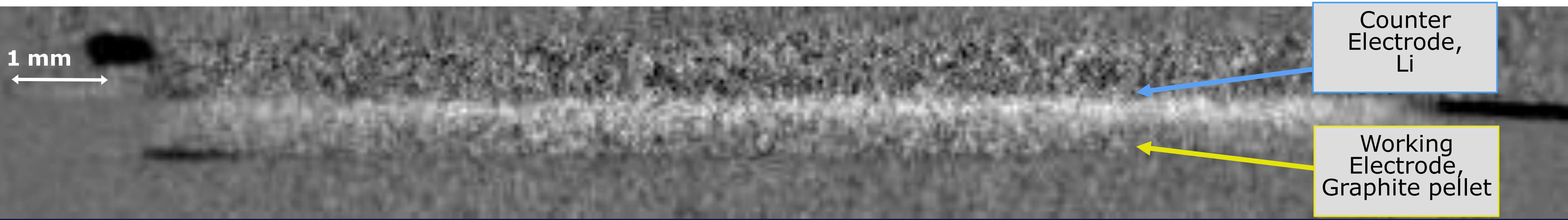

Distribution of Li and transformation $C \rightarrow LiC_{12} \rightarrow LiC_6$

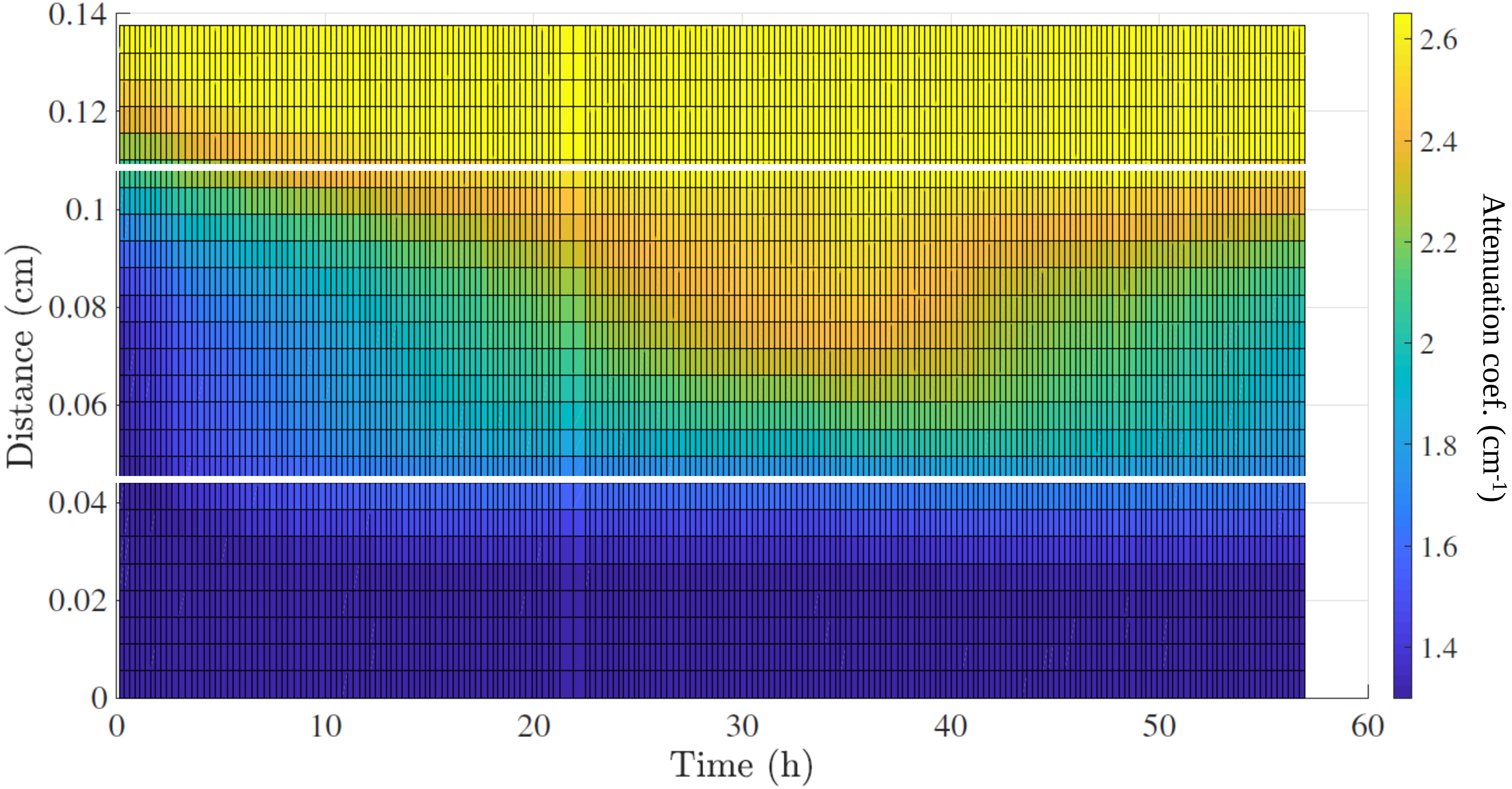

3D neutron diffraction

Reflection	d-space	Phase
0 0 2	3.355 Å	Graphite
0 0 2	3.520 Å	LiC_{12}
0 0 1	3.670 Å	LiC_6

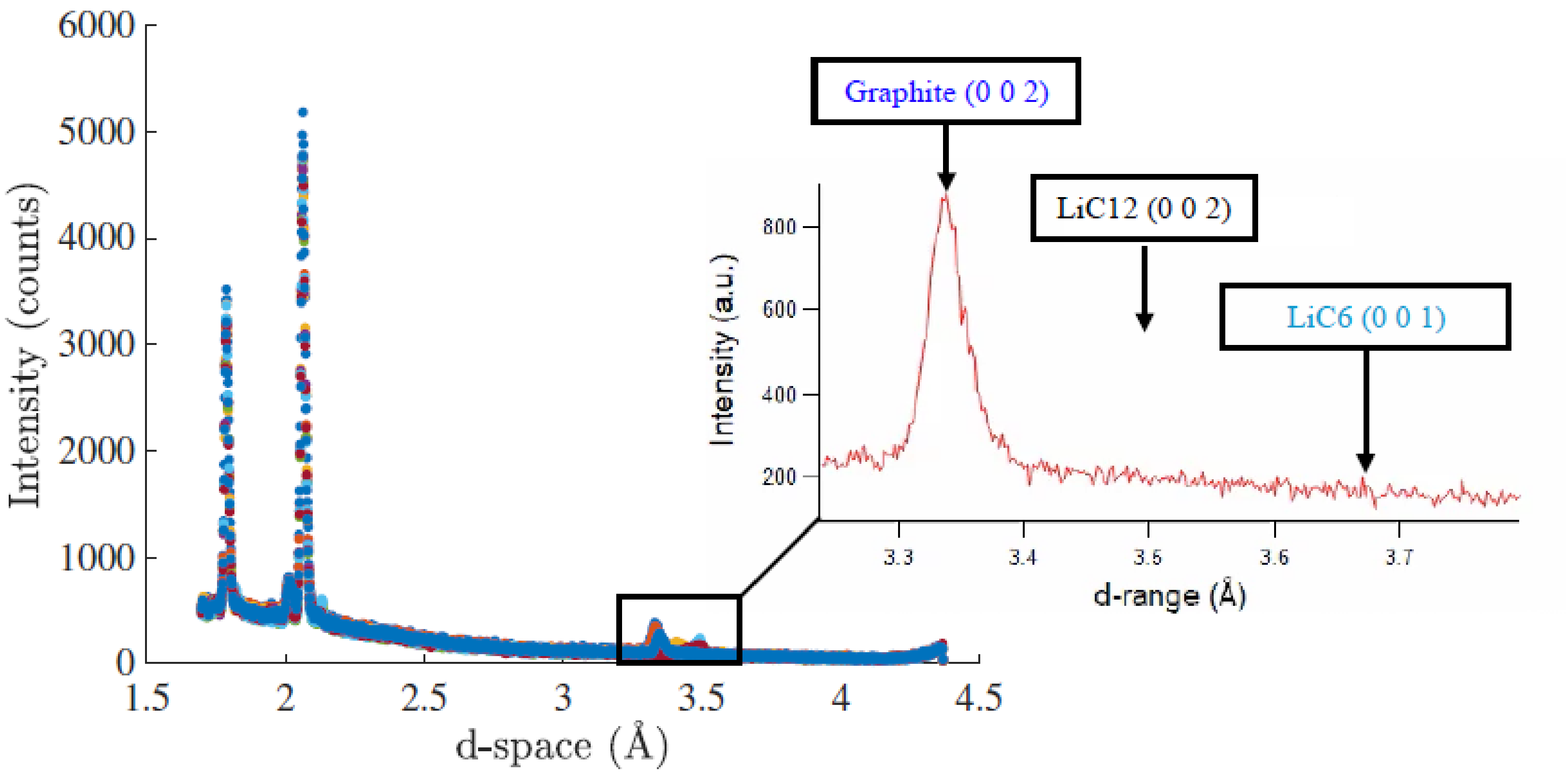

Distribution of Li and transformation C → LiC_{12} → LiC_6

Diffraction data

Imaging data

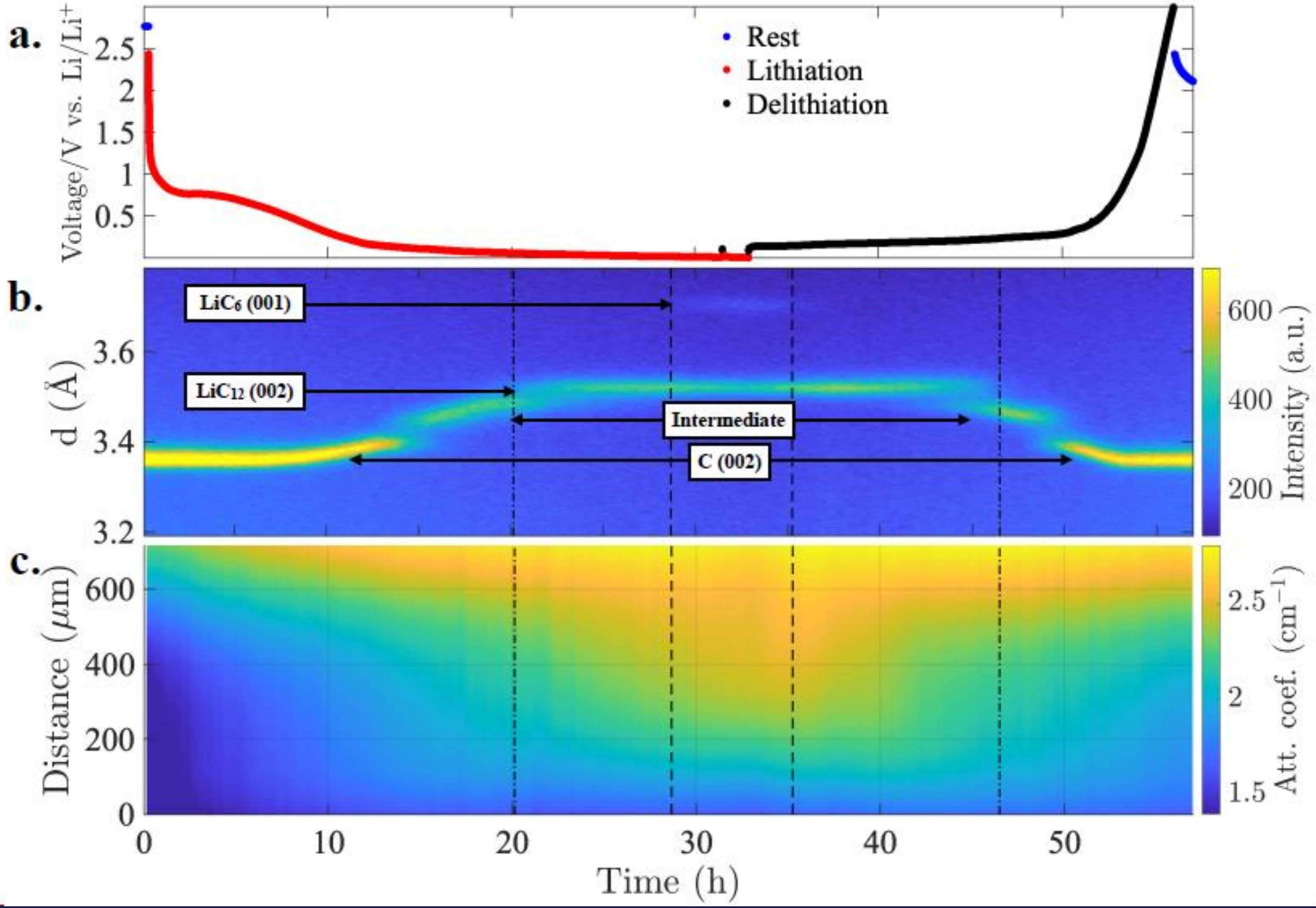

Manuscript in preparation

Enhancing contrast: Neutron grating interferometry

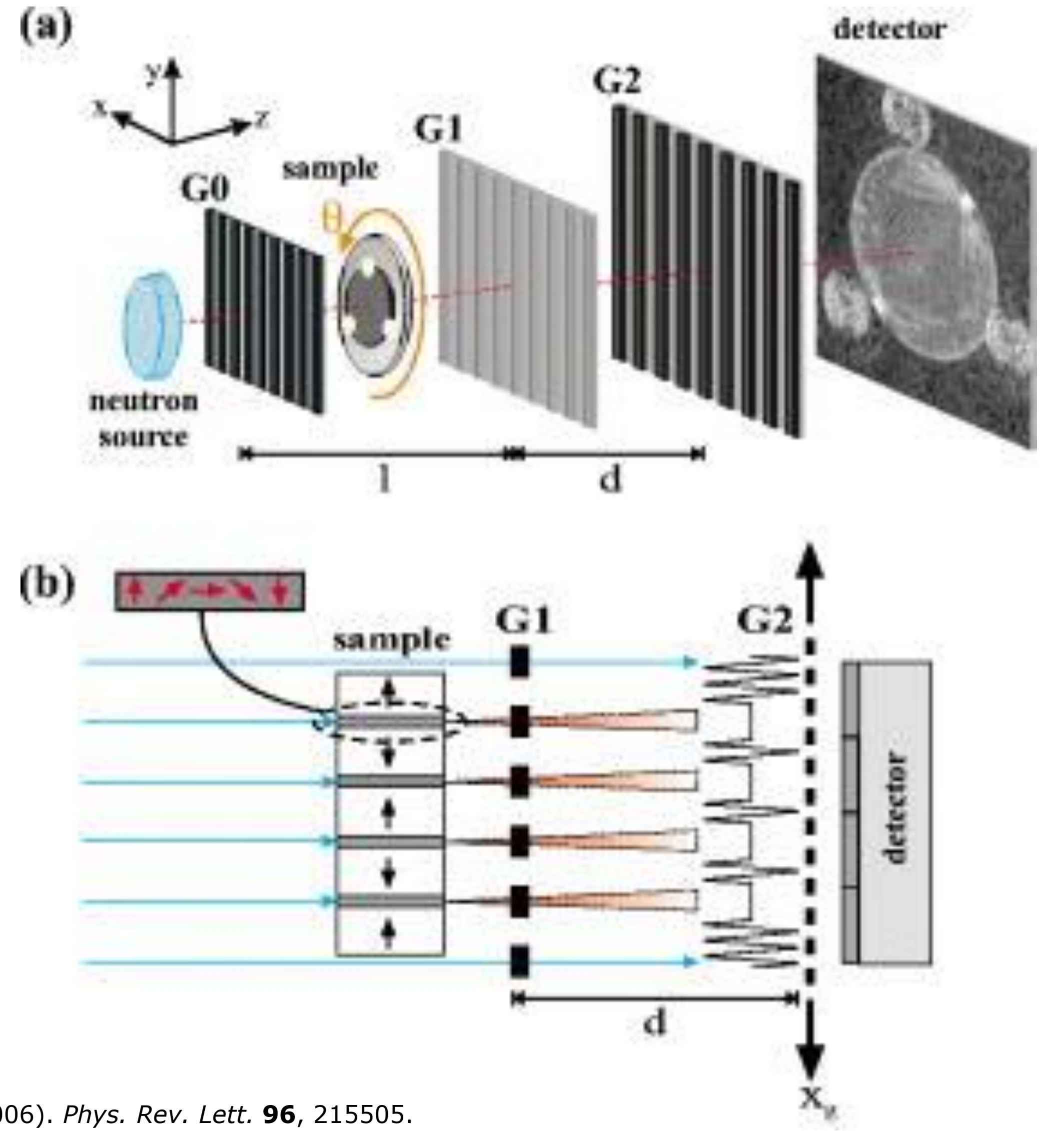

Grünzweig, C. et al. (2006). *Phys. Rev. Lett.* **96**, 215505.

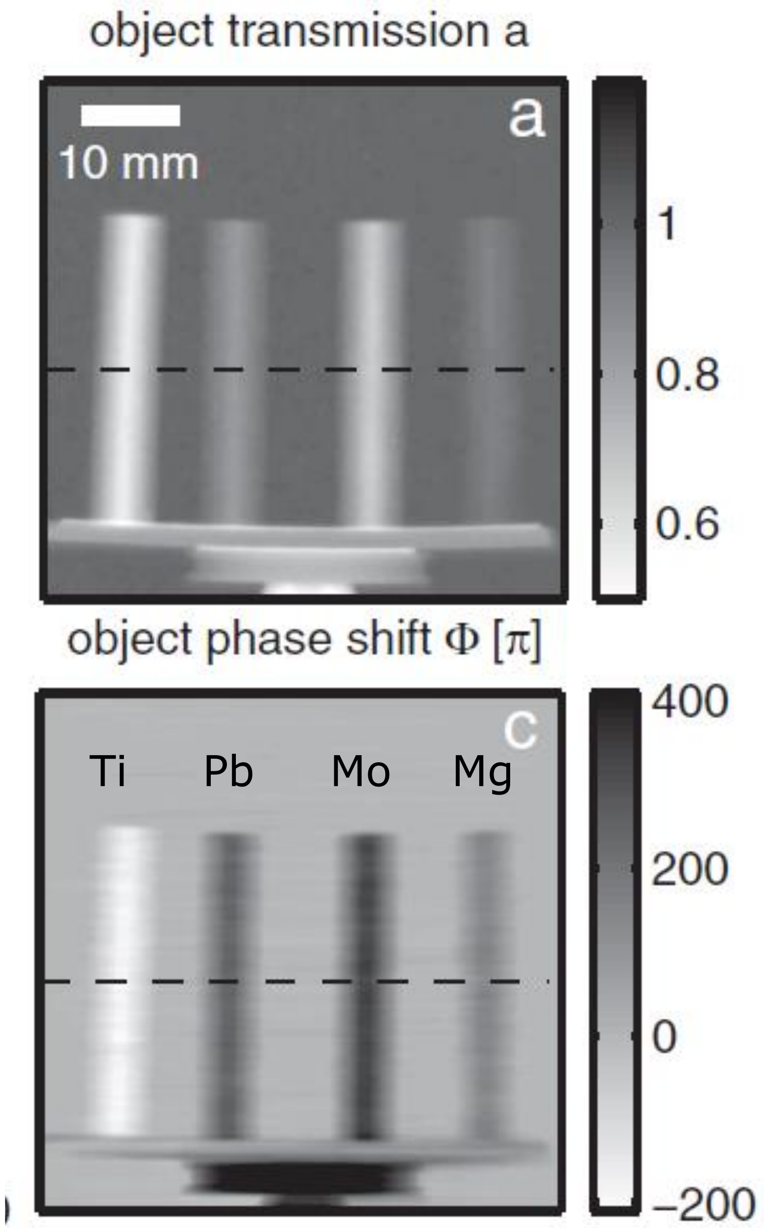

Grünzweig, C. et al. (2008). *Appl. Phys. Lett.* **93**, 112504.

3D polarimetric neutron tomography of magnetic fields and current distributions @RADEN

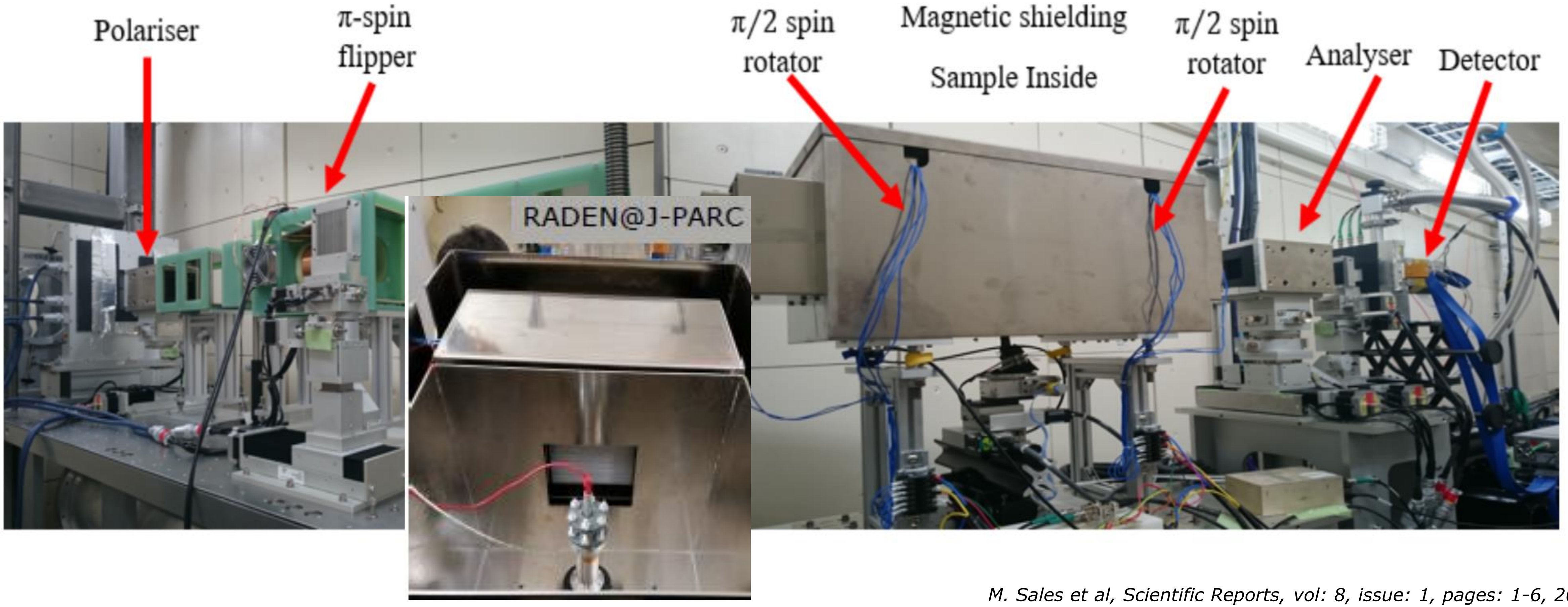

M. Sales et al, Scientific Reports, vol: 8, issue: 1, pages: 1-6, 2018

3D polarimetric neutron tomography of magnetic fields and current distributions @RADEN

(a) Structural

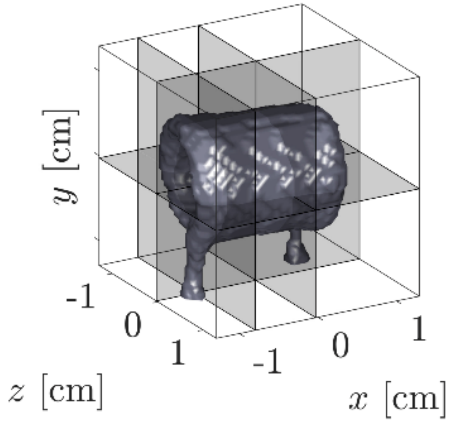

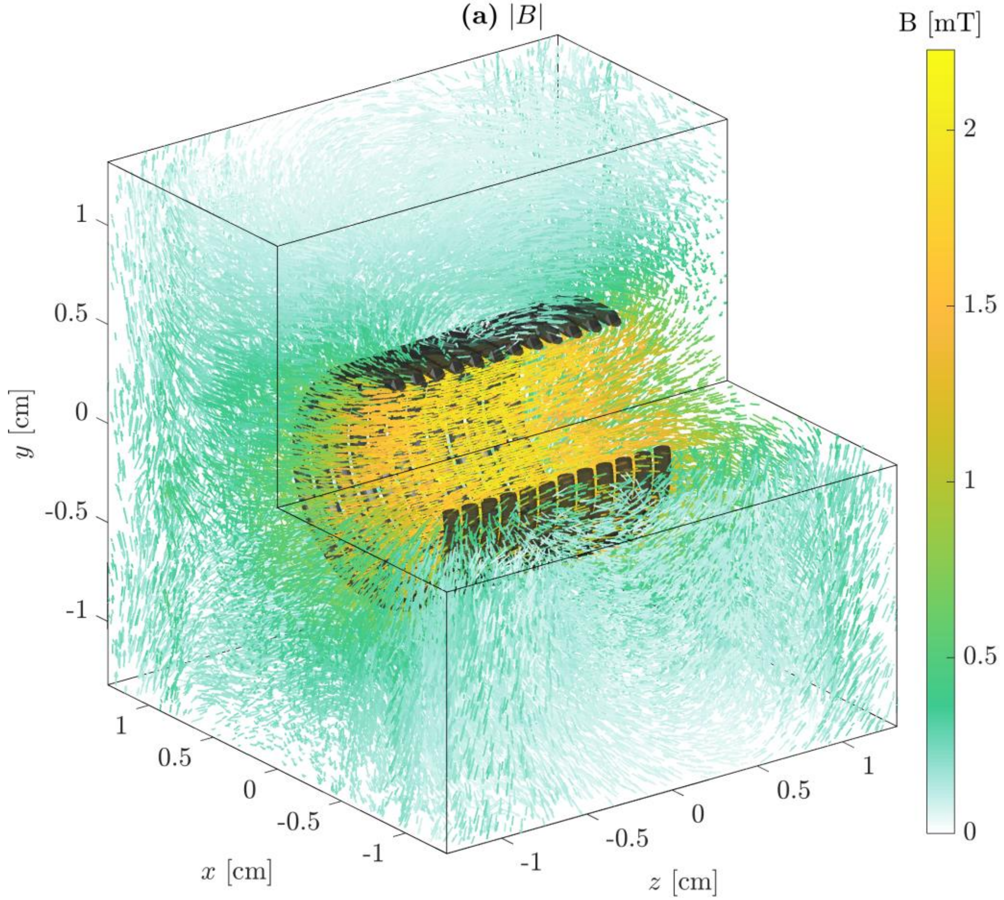

M. Sales et al, Scientific Reports, vol: 8, issue: 1, pages: 1-6, 2018

3D polarimetric neutron tomography of magnetic fields and current distributions @RADEN

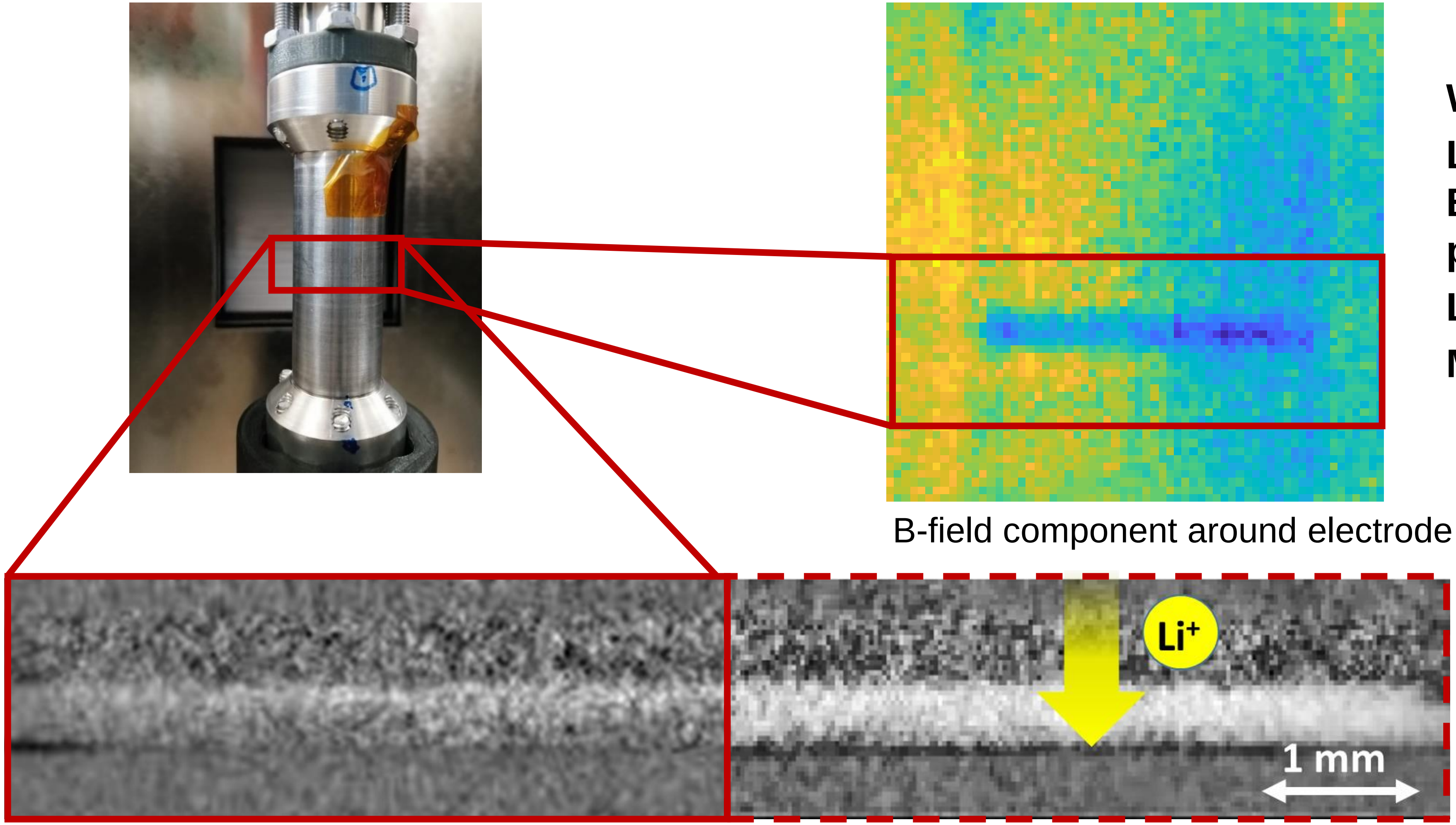

B-field component around electrode

Work in progress:

Link current distribution to Bragg-edge data in each pixel

Link to diffraction in 3D

Map in 3D

Neutron imaging

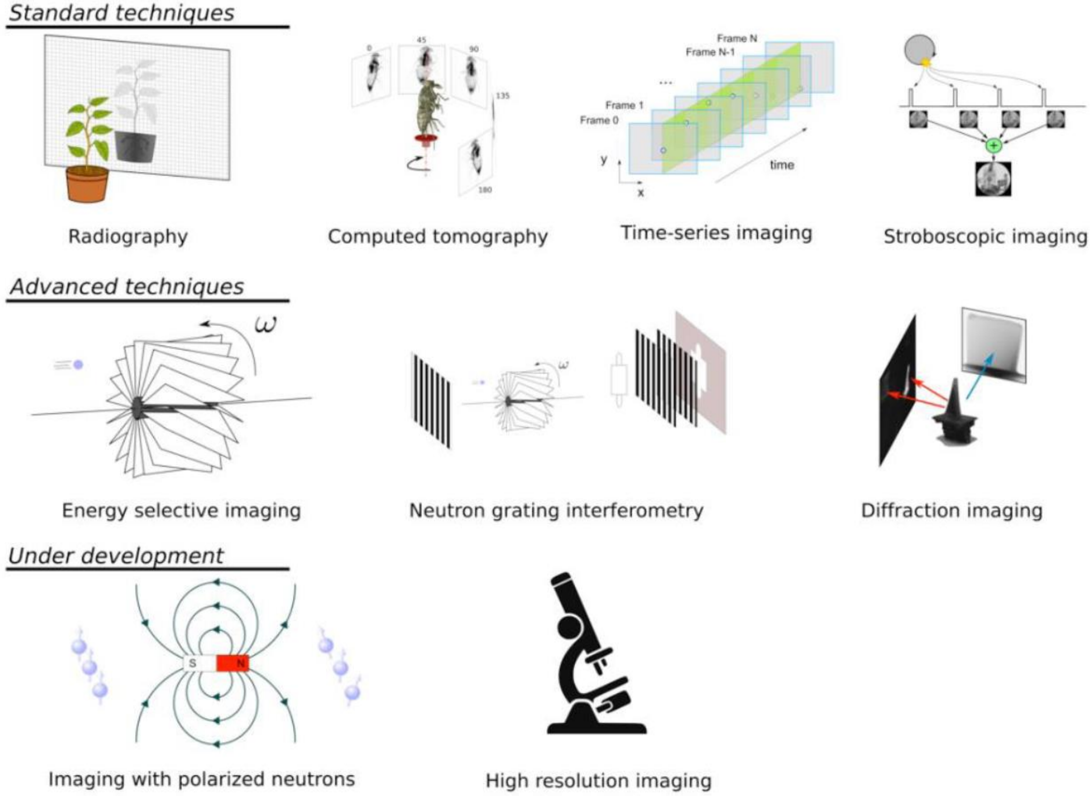

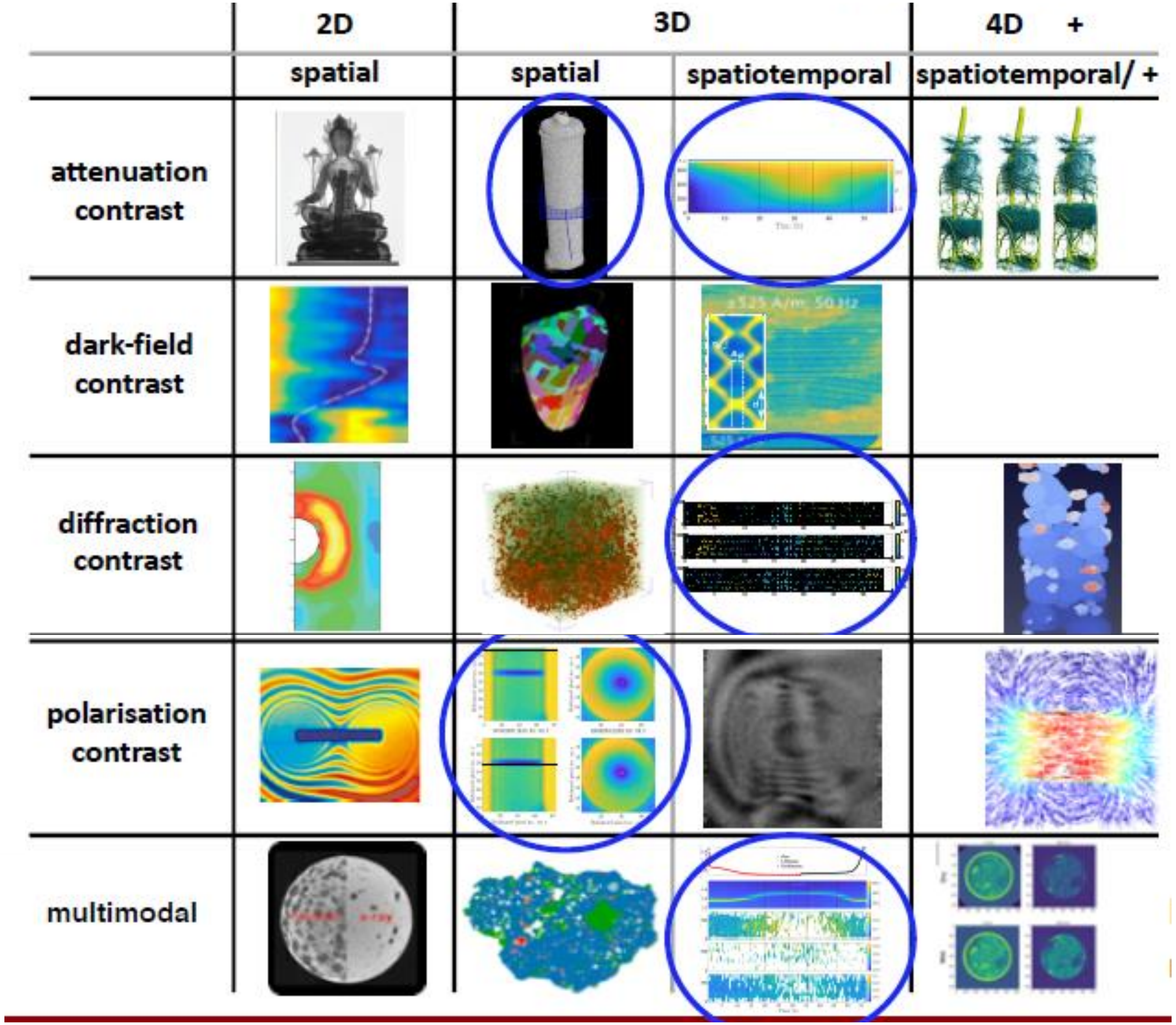

ESS: ODIN and BEER

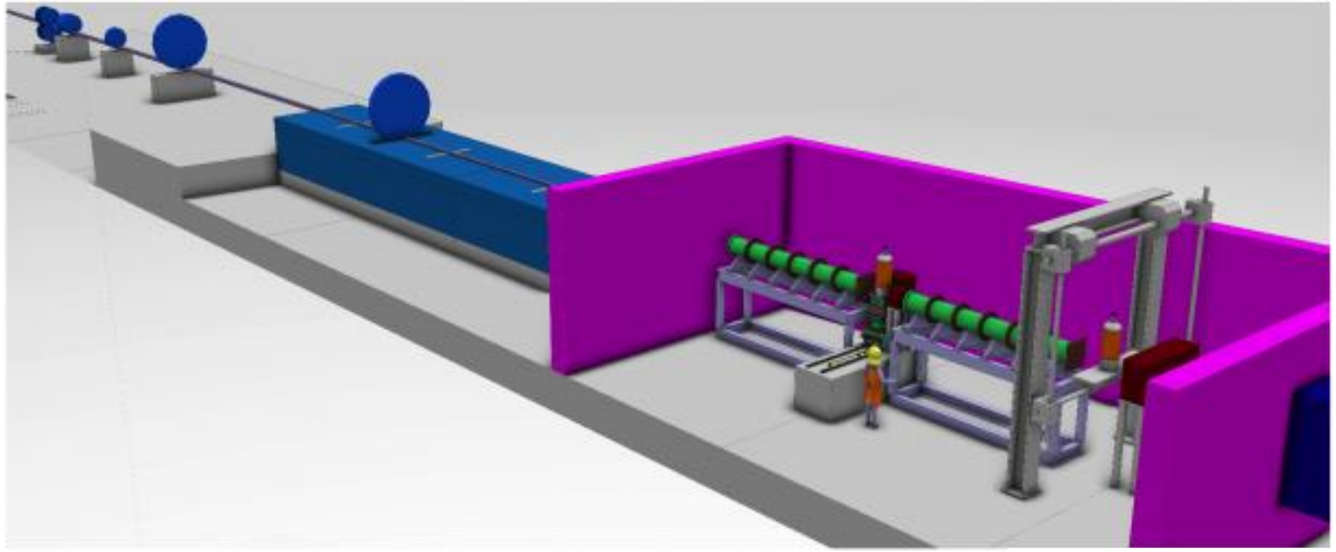

Optical and Diffraction Imaging with Neutrons - ODIN

EUROPEAN SPALLATION SOURCE

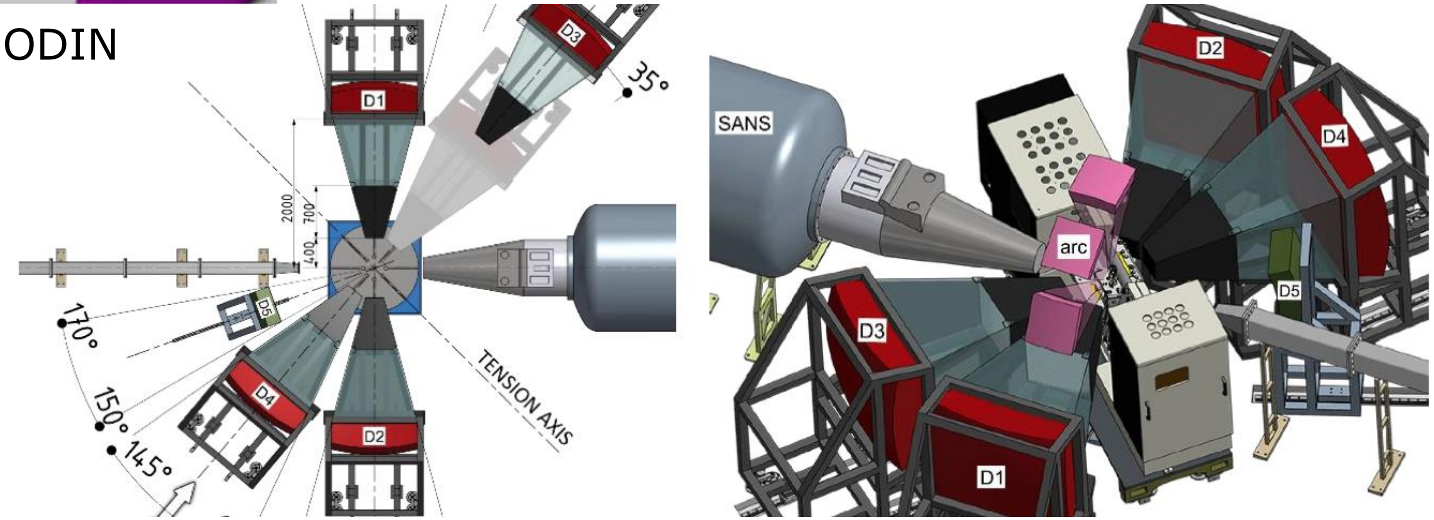

Beamline for European materials Engineering Research - BEER

Acknowledgments

DTU Energy
Department of Energy Conversion and Storage

Monica Lacatusu, Rune E. Johnsen,
Søren Koch, Mike Wichmann, John Johnson

DTU Physics
Department of Physics

Morten Sales,
Søren Schmidt

ess

Robin Woracek
Søren Schmidt

HZB Helmholtz Zentrum Berlin

Nikolay
Kardjilov

Anton Tremsin

Space Sciences Laboratory
Berkeley

J-PARC

Takenao Shinohara,
Rioji Kiyanagi

PAUL SCHERRER INSTITUT
PSI

Markus Strobl
Pavel Trtik
Manuel Morgano
Anders Kästner

The Czech Academy of Sciences

Patrick Tung,
Nancy Elewa

SUBSTANCE longterm proposal @JPARC

Interreg
Öresund-Kattegat-Skagerrak
ESS & MAX IV: Cross Border Science and Society
This project is sponsored by the European Regional Development Fund

European Union
European Regional Development Fund

NordForsk

DanScatt

Cases:
Polymer Electrolyte Membrane Fuel Cell (PEMFC)

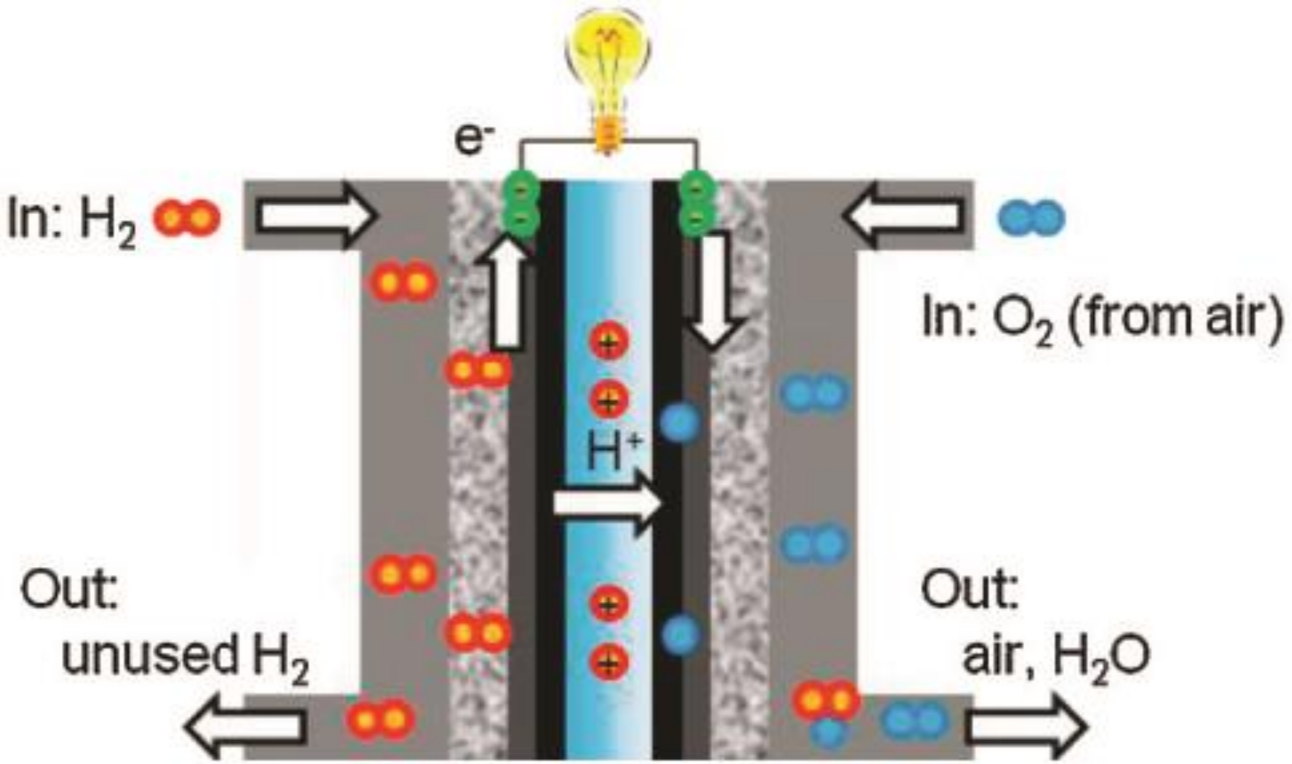

Mischler, J. et al. (2010). *Electrochimica Acta.* **75**, 1.

Cases: In-situ study of water in PEMFC

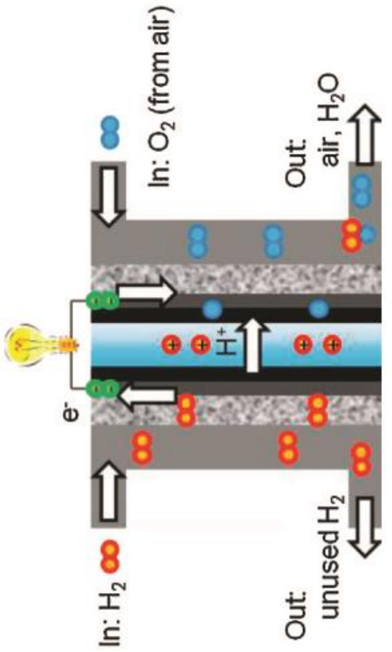

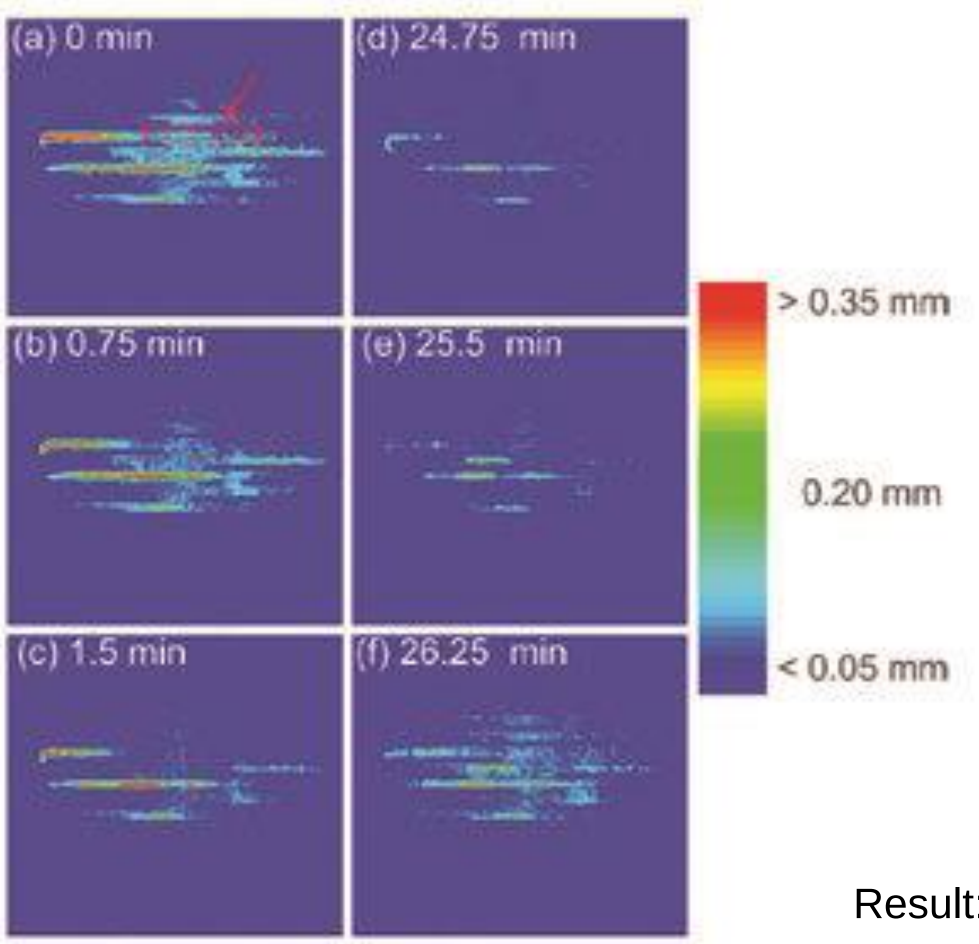

D_2

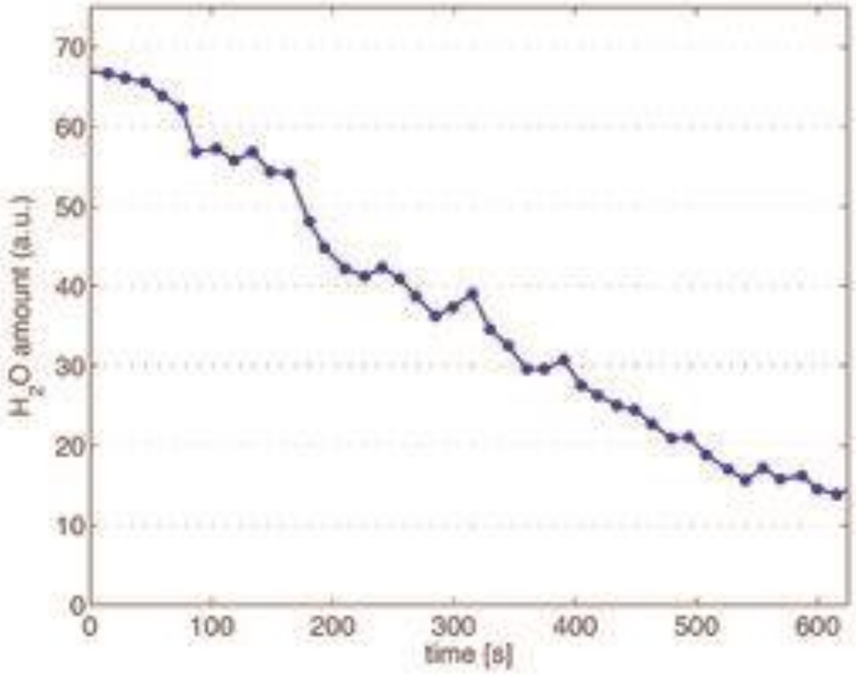

Result: a new model for two-phase flow

Manke, I. et al. (2009). *Appl. Phys. Lett.* **92**, 244101.